Experimental energy-dependent nuclear spin distributions

T. von Egidy[1] and D. Bucurescu[2,3]
[1]*Physik-Department, Technische Universität München, D-85748 Garching, Germany*
[2]*Horia Hulubei National Institute of Physics and Nuclear Engineering, R-76900 Bucharest, Romania*
[3]*Academy of Romanian Scientists, 54 Splaiul Independenţei, Bucharest, Romania*
(Received 1 August 2009; published 17 November 2009)

A new method is proposed to determine the energy-dependent spin distribution in experimental nuclear-level schemes. This method compares various experimental and calculated moments in the energy-spin plane to obtain the spin-cutoff parameter σ as a function of mass A and excitation energy using a total of 7202 levels with spin assignment in 227 nuclei between F and Cf. A simple formula, $\sigma^2 = 0.391A^{0.675}(E - 0.5Pa')^{0.312}$, is proposed up to about 10 MeV that is in very good agreement with experimental σ values and is applied to improve the systematics of level-density parameters.

DOI: 10.1103/PhysRevC.80.054310 PACS number(s): 21.10.Ma, 21.10.Hw, 21.60.−n

I. INTRODUCTION

Nuclear-level densities represent the basic statistical information on nuclei at low and especially at higher energies. The formulas for the level density are usually separated in a part with the total level density $\rho(E)$ increasing exponentially with the excitation energy E and a function for the spin distribution $f(J)$,

$$\rho(E, J) = f(J)\rho(E). \tag{1}$$

Here a possible dependence on the level parity is neglected. Two formulas are frequently used for the description of the total level density, the back-shifted Fermi gas formula (BSFG) [1],

$$\rho_{\mathrm{BSFG}}(E) = \frac{e^{2\sqrt{a(E-E_1)}}}{12\sqrt{2}\sigma a^{1/4}(E-E_1)^{5/4}} \tag{2}$$

with the free parameters a and E_1, or the constant temperature formula (CT) [1],

$$\rho_{\mathrm{CT}}(E) = \frac{1}{T}e^{(E-E_0)/T} \tag{3}$$

with the free parameters T and E_0. It was shown previously that these two level-density formulas are equivalent in many cases at excitation energies below 10 MeV [1–5]. The parameters a and T exhibit a significant shell dependence. However, this shell dependence is expected to decrease with the excitation energy. Therefore, Ignatyuk *et al.* [6] suggested an energy-dependent formula for a. Because various experiments and calculations show that this variation of a does not play a major role below 10 MeV and because our investigations concern mainly energies below the neutron binding energies, we neglect here the energy dependence of a. The spin distribution is generally proposed to be given by the formula [7]

$$f(J,\sigma) = e^{-J^2/2\sigma^2} - e^{-(J+1)^2/2\sigma^2} \approx \frac{2J+1}{2\sigma^2}e^{-J(J+1/2)/2\sigma^2} \tag{4}$$

with a single free parameter σ. It is predicted that the spin-cutoff parameter σ increases with the excitation energy E, and different energy dependencies have been used [1,6–17].

It is a task for experimental nuclear physics to determine these free level-density parameters, to investigate their systematics, and to compare them with the theoretical predictions. Level-density parameters can be obtained at low excitation energies by counting the levels in energy bins of *complete* level schemes. Another method is the fit of the integrated level-density formula to the cumulative number of levels (see Fig. 1). If no additional information (e.g., neutron resonances) is included, more than about 40 levels are required to get meaningful level-density parameters. Close to the neutron binding energy level densities are available by counting neutron resonances that have, however, only a small spin window. At higher excitation energies various nuclear reactions can be applied to determine level densities. But these methods require some theoretical assumptions and calibration procedures. In our investigations we are using complete low-energy level schemes of 310 nuclei between F and Cf (see Table I in the Appendix) and in most cases also their neutron resonance densities; this is essentially the same database that we used to determine experimental level-density parameters of formulas (2) and (3) [4] and the average low-energy spin distributions [18]. The estimation in Ref. [18] for the completeness of this set in the given energy and spin range was that 90–95% of the levels are correctly assigned. In some cases questionable spins were also accepted. Because wrong spin assignments are purely accidental, no systematic error is introduced, in particular due to the large number of used nuclei.

For the determination of the total level density $\rho(E)$ we applied a special method. The calculated level spacings $D(E) = 1/\rho(E)$ are fitted to the individual experimental spacings $S_i = (E_{i+1} - E_i)$, including the average neutron resonance spacing D_{res} (for details see Refs. [3,4]). This method avoids some problems of simple counting of levels in energy bins, because there is no binning and the final error of the parameters is well defined. It requires the range of the included spins but not all individual spins of the levels. In Ref. [4] in the BSFG case a dependence of the spin cutoff parameter σ on the level-density parameter a and excitation energy was chosen according to a formula proposed in Ref. [11]. For the CT case only an A dependence was

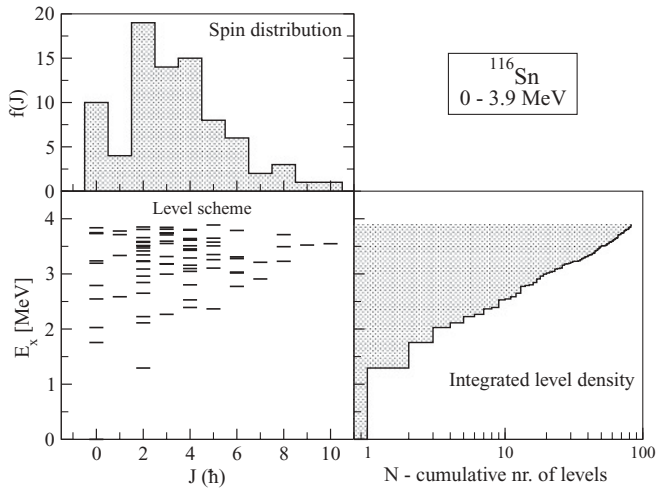

FIG. 1. (Color online) Complete level scheme of ^{116}Sn up to an excitation energy of 3.9 MeV [24,27]. The representation in the (E, J) plane and the projection on the two axes help to illustrate the method employed in the present work to deduce the dependence of the spin-cutoff parameter σ on the excitation energy.

assumed for σ, as determined from limited experimental data in Refs. [2,3]. For the experimental, empirically determined level-density parameters a, E_1 and T, E_0 we proposed simple parametrizations that use shell effects and pairing energies provided by mass tables [4].

The experimental determinations of σ are rather sparse, and in particular at higher excitation energies (above 10 MeV) there are no such determinations. At low excitation energies σ can be determined by fitting Eq. (4) to experimental spin distribution functions directly determined by counting the known discrete levels. Another method, especially useful at higher energies, is to determine σ from the anisotropy of the angular distributions of particles evaporated in various reactions such as (p, n), (α, n), (n, α), etc. There is a number of such determinations. Thus, for various nuclei between ^{48}V and ^{63}Zn, σ was determined from the (p, n) and (α, n) reactions at excitation energies generally between 3 and 10 MeV [9]. Similar measurements with the (α, n) reaction were reported for nuclei from ^{49}Cr to ^{118}Sb [19]; with the (n, α) reaction for several Cr and Fe isotopes [20] and for ^{28}Si [21]; for earlier determinations see Refs. [22,23] and citations of Ref. [9]. Systematic determinations of σ from discrete level counting were made for nuclei with mass between 20 and 41 in Ref. [14] and mass between 20 and 110 in Ref. [15], while for isolated nuclei one can give the examples of ^{116}Sn [24] and ^{112}Cd [25] and some determinations made in the present study. The potential of methods should be mentioned, devised to determine the spin values of the neutron resonances, such as the measurement of the multiplicities of the γ-ray cascades following neutron capture [26]. The σ value can be determined at the neutron resonance energy from the ratio of the numbers of resonances with two spin values.

In a recent publication [18] we evaluated the experimental spin distributions, i.e., determined the spin-cutoff parameter σ as a function of the mass number A by counting the levels in the spin groups of each nucleus. We used the same database of 310 nuclei as in Ref. [4]. In this case we neglected the energy dependence of σ to find its gross dependence on A. We observed a strong even-odd spin staggering in the spin distribution of even-even nuclei and proposed a simple formula to describe it [18]. Accordingly, the formula (4) has to be modified for even-even nuclei in the low-energy region to

$$f_{ee}(J, \sigma) = f(J, \sigma)(1 + x), \tag{5}$$

with the staggering parameter x ($x = +0.227$ for even spin, $x = -0.227$ for odd spin and $x = +1.02$ for zero spin). This effect, very probably due to pairing interactions, is predicted to disappear at higher excitation energies [16,18]. In Ref. [18] we also give a two-parameter formula that describes the A dependence of σ. However, this method is not suitable to observe the energy dependence of σ, because there are not enough levels in each spin group to separate it additionally in energy groups. Therefore, the σ values determined in this way [18] are only average spin-cutoff parameters at low excitation energies.

The main issue of this work is the presentation of a new method devised to allow a determination of the energy dependence of the spin-cutoff parameter σ from experimental level schemes. We propose a simple formula for the dependence of σ on the mass number A and excitation energy E. The next two sections present this method and a comparison of its results with experimental values and with other predictions for the dependence of σ on the mass number and excitation energy. Finally, this new prescription for σ is employed in formulas (1)–(5) to determine new level-density parameters for all 310 nuclei. The description of these new parameters by simple, global formulas is re-evaluated.

II. MOMENT METHOD TO DETERMINE THE SPIN-CUTOFF PARAMETER

As mentioned above, neither the method of counting levels in energy bins nor the fitting of formulas to the experimental level spacings is adequate to determine systematically the energy dependence of the spin-cutoff parameter. Consequently, a new method had to be developed.

Nuclear level schemes can be presented as two-dimensional graphs in the energy-spin plane (E, J). An example is given in Fig. 1 for ^{116}Sn [24,27]. The level scheme is shown in the lower left graph, its projection on the energy axis, the integrated level density, is drawn in the right side graph, while the projection on the spin axis, the spin distribution, is drawn in the upper graph. In this level scheme plane one can define momenta and compare experimental momenta with calculated ones to fit the energy-dependent spin-cutoff parameter.

Individual experimental momenta for each nucleus k are calculated with the levels i in the given energy and spin range (see Table I) with

$$M_{m,n}^{k,\mathrm{exp}} = \sum_i \left(J_i^m E_i^n\right). \tag{6}$$

For each nucleus k we are using the following nine momenta:

$$J,\ J^2,\ J^3,\ JE,\ J^2E,\ J^3E,\ JE^2,\ J^2E^2,\ J^3E^2. \tag{7}$$

The momenta E, E^2, and E^3 are not included, because it is assumed that the total level density $\rho(E)$ is known from our previous investigations and is not fitted in the present study.

The χ^2 quantity to be minimized is defined as

$$\chi^2 = \sum_k \sum_{m=1}^{3} \sum_{n=0}^{2} \left[\left(M_{m,n}^{k,\mathrm{exp}} - M_{m,n}^{k,\mathrm{calc}} \right) / dM^k \right]^2. \quad (8)$$

The calculation of the theoretical momenta $M_{m,n}^{k,\mathrm{calc}}$ is more complicated, because only average level densities and average spin distributions are available. Therefore for each nucleus the given energy range was divided into 20 equidistant pseudolevel groups, each of them containing pseudolevels with all spins of the given spin range. Consequently, the (E, J) plane is homogeneously filled with pseudolevels. For each of these pseudolevels the level density $\rho_k(E, J, \sigma)$ is calculated and normalized in such a way that the sum of all level densities in one nucleus is equal to the number of used levels in that nucleus (see Table I). The calculated momenta are obtained with the formula

$$M_{m,n}^{k,\mathrm{calc}} = \sum_{E,J} \rho_k(E, J, \sigma) J^m E^n, \quad (9)$$

where the sum goes over all pseudolevels in nucleus k. The level density $\rho_k(E, J, \sigma)$ is calculated with the CT formula (3) using T and E_0 parameters that are newly fitted to the 310 nuclei (see Table I), with the fit procedure described in Ref. [4], and somewhat simpler formulas that describe the average behavior of these parameters:

$$\rho_k(E, J, \sigma) = f(J, \sigma)(1 + x) \frac{1}{T_k} e^{(E - 0.5 P a_k')/T_k} \quad (10)$$

with

$$T_k = A^{-2/3}/(0.0570 + 0.00193 S_k') \quad \text{and}$$
$$S_k' = S_k + 0.5 P a_k'. \quad (11)$$

The term $(1 + x)$ represents the even-odd spin staggering in even-even nuclei, Eq. (5), as determined in Ref. [18] ($x = 0$ for odd-mass and odd-odd nuclei). Because this staggering is expected to decrease with increasing excitation energy [16], it is assumed that $x = 0$ at the neutron resonances. The shell energy S_k is described and tabulated in Ref. [4] and also given in Table I; it is the difference between the masses calculated with the Weizsäcker-type formula of Ref. [28] and the experimental atomic masses. Pa_k' is the deuteron pairing energy, but with a different sign definition compared to the previous value Pa_k (Ref. [29], see also the clarifications in the erratum of [4]): $Pa_k' = -(-1)^Z Pa_k$. With this definition, Pa_k' is equal in value to Pa_k tabulated in Ref. [29] and used as such in our article [4] but has reversed sign in the case of the nuclei with even Z. The use of this quantity allows us to write our formulas in a more compact and symmetric form. Pa_k' is calculated from mass or mass excess values $M(A, Z)$ of the mass tables [30] with the formula:

$$Pa_k' = \tfrac{1}{2}[M(A + 2, Z + 1) - 2M(A, Z) + M(A - 2, Z - 1)]. \quad (12)$$

The spin distribution $f(J, \sigma)$ is characterized by the parameter σ that is now considered as a function of A and E. Inspection of Fig. 1 shows that both the level density and the spin distribution do not start to increase at $E = 0$ but at an energy shifted by the pairing energy. Again we employ the deuteron pairing energy Pa_k', which has a behavior resembling in a natural way that of the energy backshifts of both BSFG and CT models, and use the following expression:

$$E' = E - 0.5 P a_k'. \quad (13)$$

We tested also whether the best pairing shift is really $-0.5 Pa_k'$ and found from fits a value of $-(0.4 \pm 0.1) Pa_k'$, so that we let it at $-0.5 Pa_k'$. We made the assumption that σ^2 is given by

$$\sigma^2 = p_1 A^{p_2} E'^{p_3} \quad (14)$$

with three free parameters p_1, p_2, and p_3.

The definition of the experimental errors is difficult, because all momentum values are correlated. A good error definition should give normalized χ^2 values close to 1.0 and deviations from the calculated values equally distributed to positive and negative values. We obtained best values with the following definition

$$dM^k = \left[\sum_{m,n} \sum_i \left(J_i^m E_i^n \right)^{1.5} \right]^{0.5}. \quad (15)$$

Other definitions of the error gave similar results but worse χ^2 values or unequal distributions of the deviations.

III. ENERGY DEPENDENCE OF THE SPIN-CUTOFF PARAMETER

For the determination of the energy dependence of the spin-cutoff parameter we used the same data set of 310 nuclei employed in our previous study [18]. Compared to our data set of Ref. [4] it was revised with new information [31] and sometimes reduced, because only levels with spin assignments were accepted. The whole set of 310 nuclei is given in Table I where one can see the energy and spin windows considered for each nucleus, as well as other quantities of interest. The procedure described in the previous section was applied only to nuclei with at least 18 levels with spin assignments (to ensure a meaningful spin and energy information) that gave a total of 7202 levels with spin assignment in 227 nuclei.

The result of the fit with the procedure described above, for the parameters in Eq. (14) is $p_1 = 0.391 \pm 0.025$, $p_2 = 0.675 \pm 0.014$, and $p_3 = 0.312 \pm 0.011$, that is:

$$\sigma^2 = 0.391 A^{0.675} (E - 0.5 P a')^{0.312}. \quad (16)$$

We made the similar fit for only even-even, odd, or odd-odd nuclei and found essentially the same parameters, confirming that this parametrization is independent of these structure differences. In our previous investigation of the spin-cutoff parameter without energy dependence [18] we obtained the result $\sigma^2 = 2.61 A^{0.28}$. The reason for the previously weaker A dependence is the fact that our data set contains many light nuclei with levels up to high excitations (and large positive

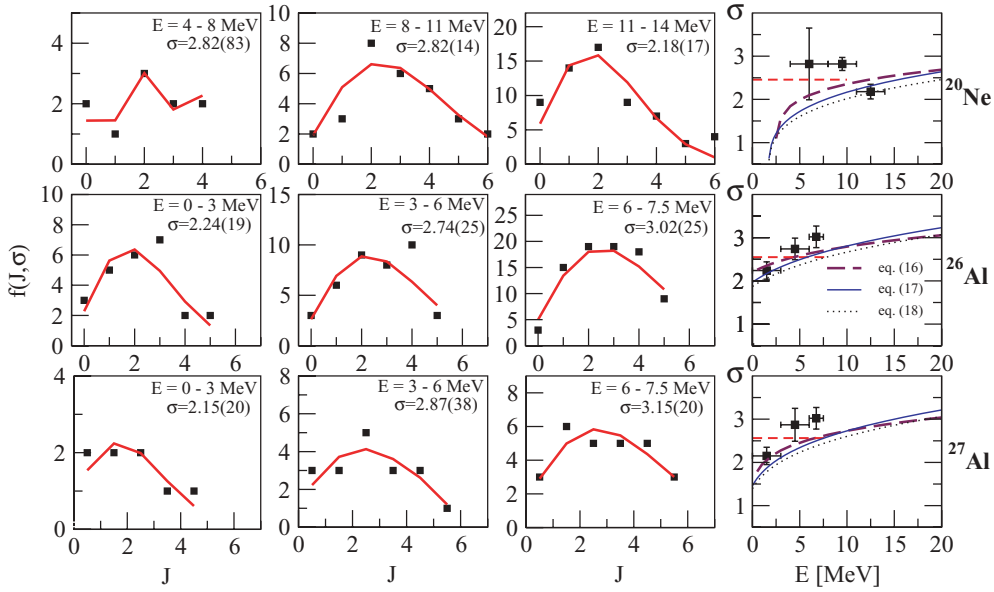

FIG. 2. (Color online) Comparison of experimental spin distributions and σ values with those provided by the empirical formula (16) and formulas (17) and (18), for three nuclei with mass ∼20. For the even-even nuclei, at low excitation energies, we employ the odd-even spin staggering evidenced in Ref. [18] (see text). The left-side graphs show spin distribution functions for different excitation energy ranges determined from the known complete level schemes [31], and the right-side graphs the resulting σ values (symbols) compared to the predictions (curves). The horizontal dashed line shows the low-energy σ value provided by our empirical formula from Ref. [18]: $\sigma^2 = 2.61A^{0.28}$.

pairing shifts for odd-odd nuclei) where the energy dependence plays a major role, thus increasing the average σ values. As it will be shown in the figures that follow, these average low energy values are also in good agreement with experiments.

Due to the nucleon orbitals near the ground state there is sometimes a strong preference of one parity at low excitations. However, the total level density increases relatively smoothly because the nuclear potential depends mainly on mass number A and less on the shells. Consequently, in looking for smooth functions of the level density it is not meaningful to include a parity dependence and we neglected it in the present work. Also, on the basis of a microscopic BCS Hamiltonian approach, a dependence of σ on the shell structure near the Fermi energy was claimed [32]. We checked an additional shell-dependence term of the type $[1 + p_4(S + 0.5Pa')]$ in our formula (14) and the resulting value of p_4 was found zero, consequently the shell dependence is very weak.

Most of the theoretical predictions for the spin-cutoff parameter σ are based on the expression derived by Ericson [7] within the Fermi gas model

$$\sigma^2 = gt\langle m^2\rangle,$$

where g is the density of single-particle states, related to the level-density parameter a by $g = 6a/\pi^2$; t is the temperature, related to the excitation energy E by $t = \sqrt{(E-\delta)/a}$; and $\langle m^2\rangle$ is the average of the square of the spin projection on the z axis for the single-particle states near the Fermi level. One of the most common predictions, based on a statistical mechanical calculation of $\langle m^2\rangle$ using appropriate single-particle states is [33]

$$\sigma^2 = 0.1461\sqrt{a(E-\delta)}A^{2/3}. \quad (17)$$

Another frequently refered to formula is based on the assumption that the nucleus is a rigid sphere of radius $R = 1.25A^{1/3}$ fm that yields [9]

$$\sigma^2 = 0.0145\sqrt{(E-\delta)/a}A^{5/3}. \quad (18)$$

Reference [15], which continues and develops the work of Ref. [14], studied systematically the variations of the parity ratio and of the spin cutoff parameter with the mass number and excitation energy. In this work, level densities

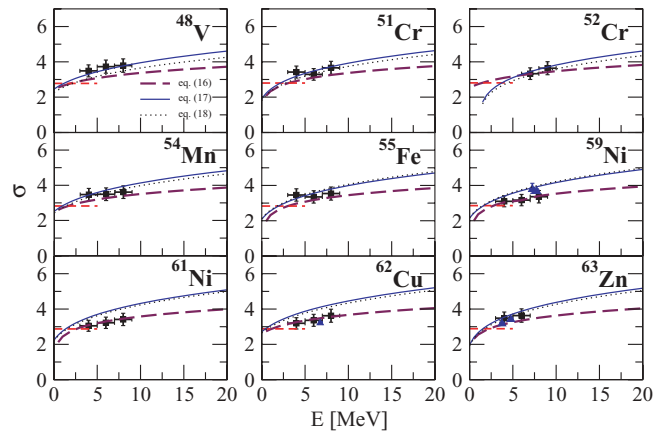

FIG. 3. (Color online) Similar to the right side of Fig. 2 for σ values of various $A \sim 60$ nuclei from Ref. [9]. The triangles are determinations from Ref. [19].

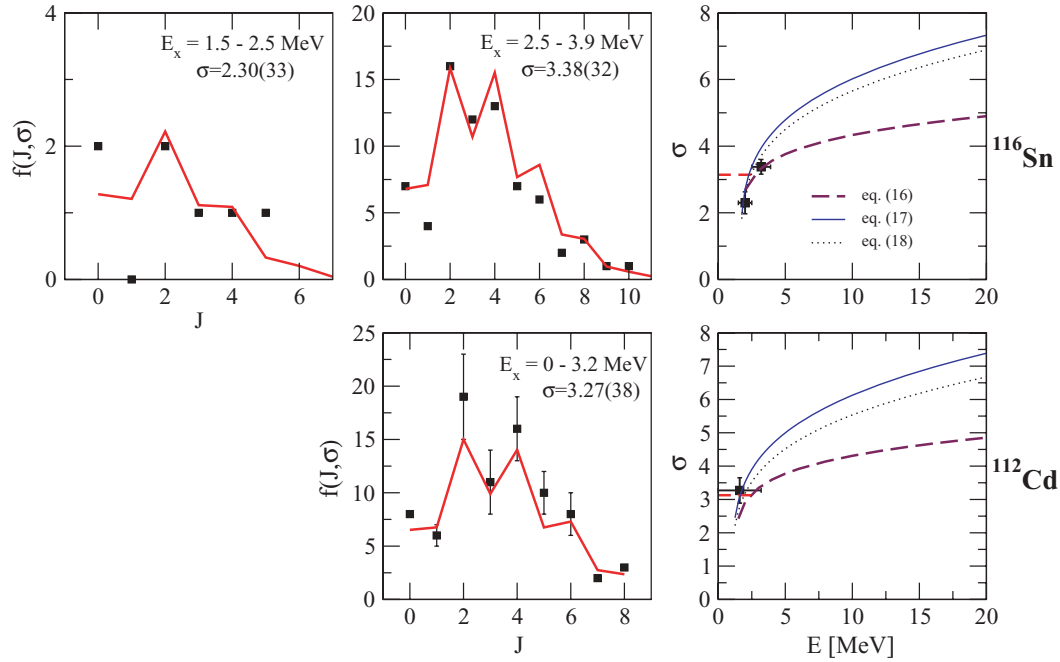

FIG. 4. (Color online) Similar to Fig. 2 for σ values determined from low-energy level schemes of ^{116}Sn [24] and ^{112}Cd [25].

were studied within the BSFG model for nuclei mainly in the mass range 20 to 110 (several nuclei up to mass 140 were also included) by looking at the known low-energy levels. Several simple parametrizations were proposed for the level-density parameter a as a function of A and Z, and for the energy shifts as a function of the shell correction. As for the spin-cutoff parameter, both formulas (17) and (18) were checked, and it was found that they fit reasonably well the existing data, with numerical constants (resulting from fit) close to the theoretically expected ones of 0.1461 and 0.0145, respectively. For example, by fitting the data with the "rigid body"-type of formula (18), $\sigma = ct(E-\delta)^{1/4}A^{5/6}a^{-1/4}$, the values determined for the parameter ct are found to decrease with A, in average, like $ct = 0.10578 - 0.000202A$. This indicates σ values slightly smaller than the rigid body values (18) especially at the higher masses.

The main result of the present work, that is Eq. (16), will be compared now with different experimental measurements

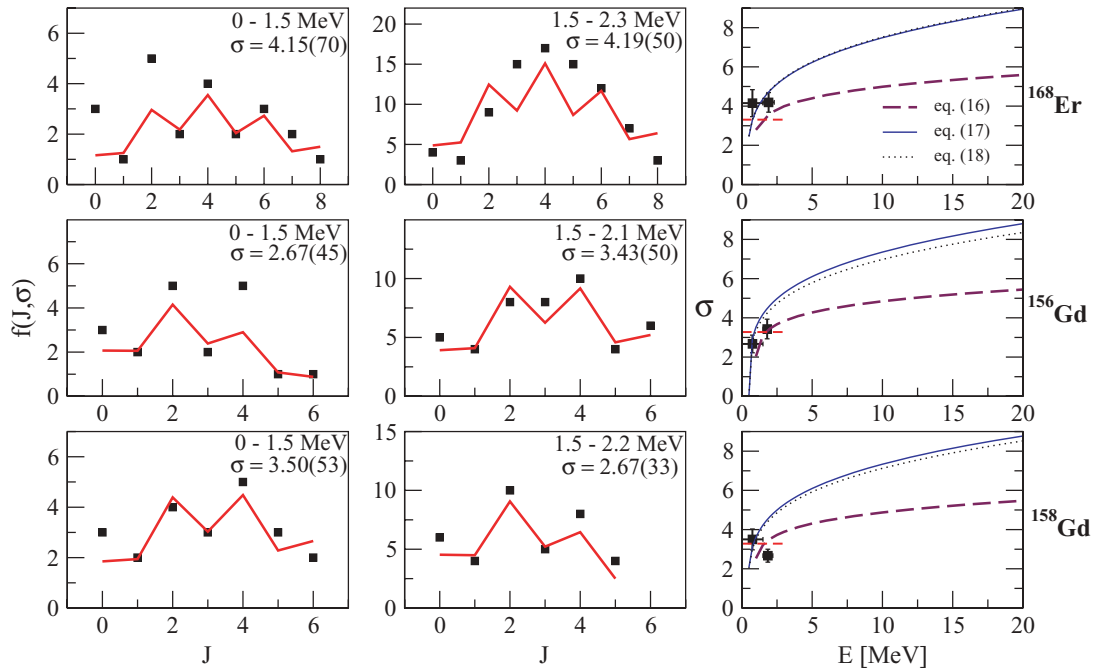

FIG. 5. (Color online) Similar to Fig. 2 for σ values determined from complete low-energy level schemes of three $A \sim 160$ nuclei.

of σ and other theoretical predictions. In the figures that follow we compare first the predictions of formula (16) with different experimental determinations. In all these figures the predictions of Eqs. (17) and (18) are also shown for comparison. They were calculated by using for the parameters a and δ (the energy backshift E_1) values obtained in this work (from level-density fits, Sec. IV) and given in Table II or calculated with the average formulas (19) and (20) outlined in Sec. IV; these values do not differ much from those previously published [4]. Figure 2 shows three light nuclei ($A \approx 25$) with experimental σ values determined by us from level counting. We emphasize that in the case of the even-even nuclei there is an even-odd spin staggering in the spin distribution function at low excitation energies [18]. Figure 3 shows a comparison with experimental σ values deduced from evaporated particle angular distributions for nuclei in the $A \approx 60$ region [9,19]. Figure 4 presents the σ values determined from the level schemes of ^{116}Sn [24] and ^{112}Cd [25]. In Fig. 5 three nuclei in the $A \sim 160$ region are shown. For these nuclei we determined experimental σ values from their complete low-energy level schemes up to the excitation energies indicated in each case.

From Figs. 2–5 one can see that in most cases formulas (16), (17), and (18) give similar predictions at the lower excitation energies, in reasonable agreement with the available experimental data. At higher energies, Eq. (16) starts to differ from the predictions of formulas (17) and (18), the latter two showing generally similar trends. The statistical model formula (17) seems to be closer to the data than the "rigid-body" formula (18). Equation (16) of the present work appears to describe better the existing data for the lighter mass nuclei. This is especially obvious in Fig. 6 where the three formulas are compared to experimental data for ^{28}Si [21] and ^{24}Mg [34]. In both cases, predictions of microscopic Fermi gas calculations using appropriate single particle levels near the Fermi level, are also shown in Fig. 6 (similar predictions are compared with experimental data for many nuclei with mass between 20 and 41 in Ref. [14]). In the same figures (2 to 5) one can see that formula (16) gives σ values in good agreement with the ones determined in our previous work [18] ($\sigma^2 = 2.61A^{0.28}$).

For higher excitation energies (above 10 MeV) we can compare formula (16) only with other theoretical predictions. Figure 7 shows such a comparison with microscopic calculations of σ for ^{152}Sm based on a static path approximation representation of the partition function for a pairing-plus-quadrupole interaction model Hamiltonian [13]. Figure 8 shows the same type of comparison, with the SMMC (shell-model Monte Carlo) calculations [16] for the nuclei ^{55}Fe, ^{56}Fe, and ^{60}Co. The two predictions are rather comparable in the low energy region (below about 7 MeV) and start to differ at higher energies. Rather conspicuously, the SMMC results are very similar to those calculated with formulas (17) and (18). Next, we show a comparison with results of very large scale shell-model calculations, as calculated with the method outlined in Ref. [35]. Figure 9 shows this comparison for ^{28}Si, as calculated in the sd-shell model space [36]. Both the results of exact calculations and of an approximate (zeroth-order) approach [36] are shown. At higher excitation energies Eq. (17) is the closest to the "exact" calaculations, while Eq. (16) is

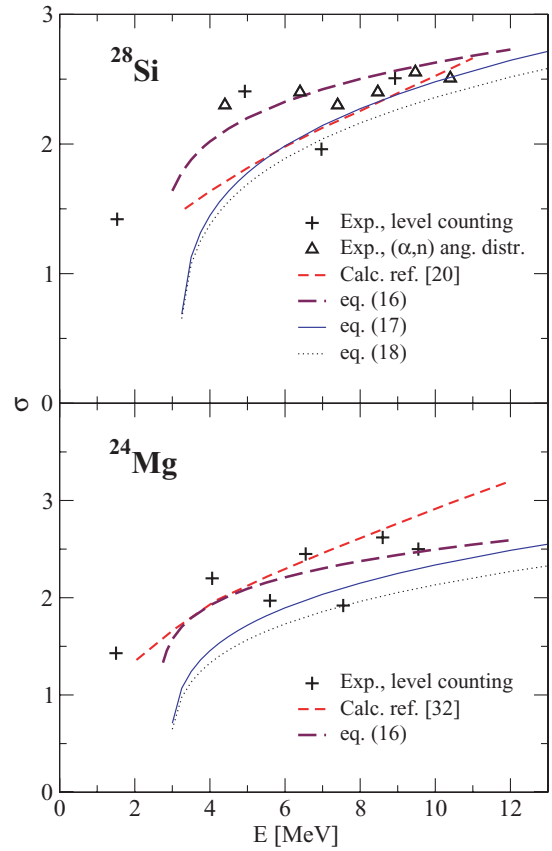

FIG. 6. (Color online) Comparison of the predictions of formulas (16), (17), and (18) for ^{28}Si and ^{24}Mg, with experimental data (symbols) and microscopic Fermi gas calculations with appropriate single-particle states (dashed curves). Experimental data are from Refs. [21,34]. The dashed curves were extracted from Ref. [21] for ^{28}Si, corresponding to the curve labeled "Seeger-Howard" in their Fig. 3, and from Ref. [34] for ^{24}Mg, corresponding to the curve labeled "Seeger-Perisho" in their Fig. 2.

closer to the approximate SM calculation; however, at the lower energies, Eq. (16) describes best the data (as remarked before, Fig. 6). We are not aware of other predictions of σ values that could be directly compared to our experimental formula.

One should note that the present result, represented by Eq. (16), offers an alternative to the "classical" formulas (17) and (18), for the determination of the spin-cutoff parameter. The later formulas depend on the knowledge of the BSFG level-density parameters, therefore for nuclei for which these cannot be determined from experimental data one must rely on different types of prediction for these parameters. By contrast, the approach presented in this work provides the empirical formula (16), which contains a direct dependence on mass A and excitation energy E, and, through the backshift utilized ($0.5Pa'$), also an implicit dependence on the type of the nucleus (even-even, odd-A, or odd-odd), thus distinguishing between isobars. Due to the scarcity of experimental data we cannot make a general statement concerning the performance of formula (16) proposed in the present work, but, because it is based mainly on low-energy discrete levels, we can say that

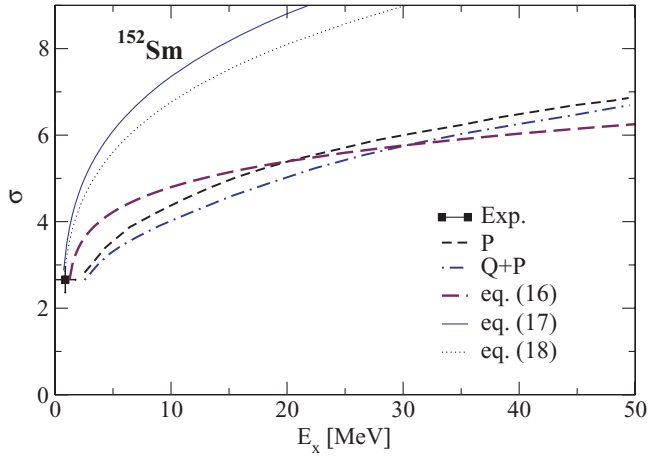

FIG. 7. (Color online) Comparison of formulas (16), (17), and (18) for ^{152}Sm with predictions of microscopic calculations with a pairing+quadrupole interaction Hamiltonian [13]. The rectangle symbol at low energy is an experimental determination of σ from the complete level scheme up to 1.77 MeV.

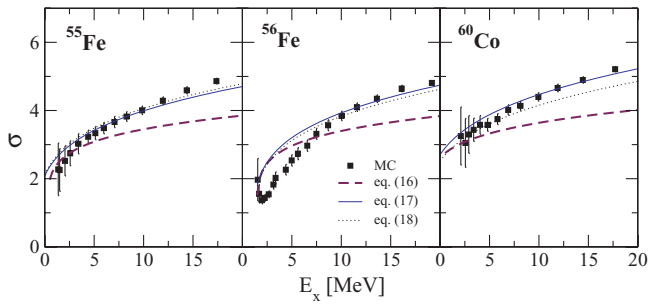

FIG. 8. (Color online) Comparison of formulas (16), (17), and (18) with shell-model Monte Carlo predictions (symbols) [16] for ^{55}Fe, ^{56}Fe, and ^{60}Co.

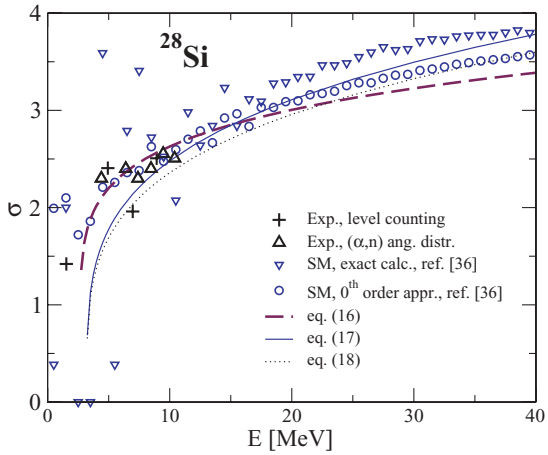

FIG. 9. (Color online) Comparison of formulas (16), (17), and (18) with large shell-model calculations for ^{28}Si ([36]). The experimental data from Ref. [21] are also shown.

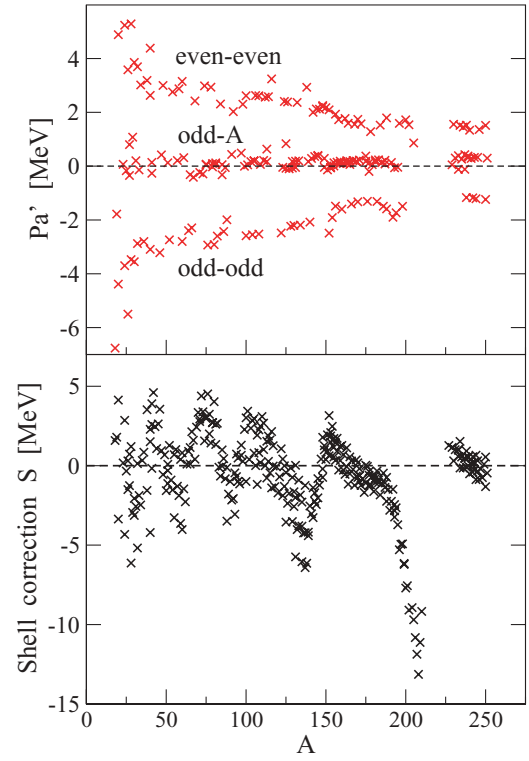

FIG. 10. (Color online) The deuteron pairing Pa' [formula (12)] and the shell correction S (difference between the mass calculated with the Weizsäcker-type formula [28]) and the experimental mass for the 310 nuclei as given in Table I. Note that the quantity Pa' [Eq. (12)] differs from Pa used in Ref. [4] and tabulated in Ref. [29] by a factor of $(-1)^{Z+1}$.

at energies up to about the neutron binding energy it may be one of the most realistic proposals.

IV. RE-EVALUATION OF THE LEVEL-DENSITY PARAMETERS

In our previous work [4] we determined the parameters a and E_1 of the BSFG model [Eqs. (1) and (2)], and T and E_0 [Eqs. (1) and (3)], by fitting experimental level spacings and the average neutron resonance spacings for the 310 nuclei in our data set (the level density at the neutron binding energy did not exist for only 14 light nuclei—see Table I in the Appendix—but we still considered these nuclei in the fit because their complete level scheme was known up to rather high energy). For the BSFG, we used an expression for the spin-cutoff parameter σ that was proposed in Ref. [11], which contained a certain dependence on the excitation energy. For the CT model, however, we used an older prescription [3] for σ that depended on the mass number but actually did not contain any energy dependence.

In the present work we propose the empirical formula (16) for the dependence of σ on both mass and excitation energy, which was derived from the experimental data on the nuclear level schemes of 227 nuclei from our set that had at least 18 levels with known spin. Using this experimental determination of the spin distribution function (4), we found now new

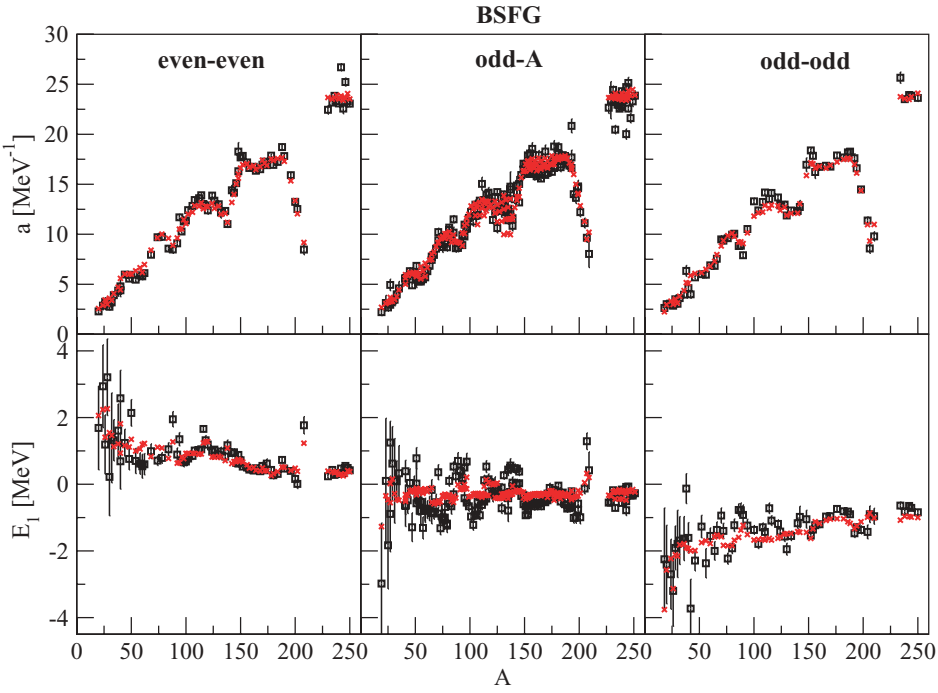

FIG. 11. (Color online) The new level-density parameters for the BSFG model (Table II). The rectangles with errors are the empirically determined values, while the x symbols are the fits with formulas (19) and (20).

level-density parameters for the BSFG and CT models for all 310 nuclei from our data set, revised as given in Table I (Appendix). The procedure is identical with that described in Ref. [4], except that for σ in Eq. (4) we use the values given by the empirical formula (16), and for even-even nuclei we include the term $(1 + x)$ [see Eq. (5)] to take care of the even-odd spin staggering [18].

The level-density parameters thus obtained are given in Table II from the Appendix. They are only slightly different from those of Ref. [4]. Following the lines of our previous article [4] we have described these empirical parameters with simple formulas, which emphasize strong correlations between these parameters and quantities such as the shell correction and the deuteron pairing. Figure 10 displays these two basic quantitites: the deuteron pairing Pa' and the shell correction. Especially the deuteron pairing defined by Eq. (12) is remarkably similar to the backshift energies empirically determined.

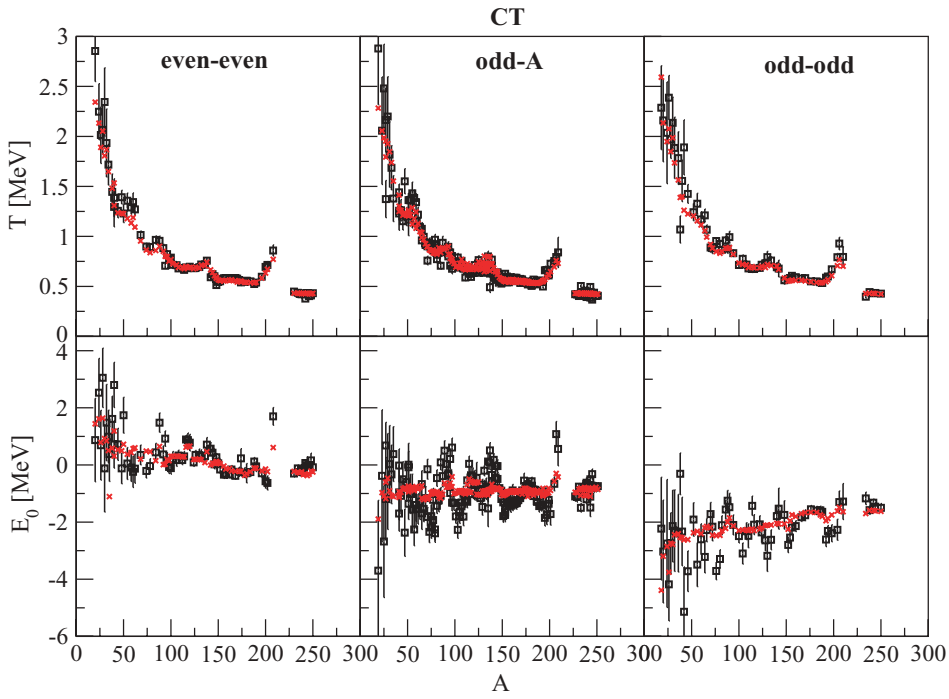

FIG. 12. (Color online) The new level-density paramaters for the CT model (Table II). The rectangles with errors are the empirically determined values, while the x symbols are the fits with formulas (21) and (22).

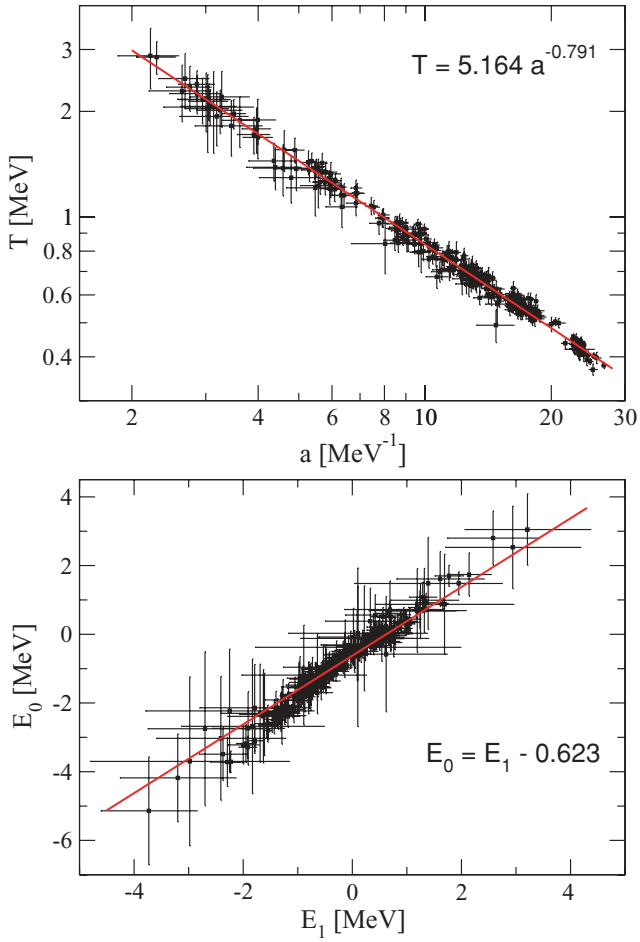

FIG. 13. (Color online) Correlations between the newly determined level-density parameters (Table II) of the BSFG and CT models. The line drawn in the lower graph is the straight line resulting from relations (20) and (22).

Thus, for the BSFG parameters, we propose the following formulas:

$$a = (p_1 + p_2 S')A^{p_3} = (0.199 + 0.0096S')A^{0.869}, \quad (19)$$

with $S' = S + 0.5Pa'$, and $p_1 = 0.199(7)$; $p_2 = 0.0096(4)$; $p_3 = 0.869(7)$.

$$E_1 = q_1 + 0.5Pa' = -0.381 + 0.5Pa', \quad (20)$$

with $q_1 = -0.381(14)$.

The experimental values of a and E_1 and their fits with formulas (19) and (20) are shown in Fig. 11.

For the CT parameters we obtain the following formulas:

$$T = A^{-2/3}/(p_1 + p_2 S') = A^{-2/3}/(0.0597 + 0.00198S'), \quad (21)$$

with $S' = S + 0.5Pa'$ and $p_1 = 0.0597(2)$; $p_2 = 0.00198(10)$.

$$E_0 = q_1 + 0.5Pa' = -1.004 + 0.5Pa', \quad (22)$$

with $q_1 = -1.004(21)$. Separate fits for even-even, odd, and odd-odd nuclei gave very similar results. In the very simple approximations for the backshifts E_1 and E_0 [Eqs. (20) and (22)] we neglected the term dS/dA used in Ref. [4], because this was only a very rough approximation of the fluctuations of E_1 and E_0 in odd and odd-odd nuclei.

The experimental values of T and E_0 and their fits with formulas (21) and (22) are shown in Fig. 12.

It was shown in Ref. [37] that there are very compact correlations between the parameters of the BSFG and CT models. The newly determined parameters are also well correlated, as shown in Fig. 13. The fit in the upper graph corresponds to the relation

$$T = 5.164a^{-0.791}, \quad (23)$$

while for the energy backshifts a linear relationship results from Eqs. (20) and (22):

$$E_0 = E_1 - 0.623, \quad (24)$$

which is seen to describe reasonably well the observed correlation (Fig. 13). These relations are similar to those obtained [37] for the old parameters from Ref. [4].

V. CONCLUSIONS

We determined for the first time the empirical mass and energy dependence of the spin-cutoff parameter σ in a broad mass range from F to Cf. A surprisingly simple formula [Eq. (16)] with only three parameters was found that reproduces the existing experimental σ values rather well. Both the mass dependence and the energy dependence of σ are significantly less than the theoretical predictions. The formulas (17) and (18) yield for σ^2 an A dependence of about $A^{1.2}$ and an energy dependence of about $(E - E_{\text{pairing}})^{0.5}$, while our investigation gives exponents of about 0.7 and 0.3, respectively.

With the new formula for σ^2 the level-density parameters of the BSFG and CT models were determined again for the set of 310 nuclei used in Ref. [14]. These new parameters are very similar to the ones obtained previously [14]. This indicates that the extraction of level-density parameters is largely independent of the assumed spin distribution. The BSFG and CT formulas reproduce the experimental level densities at low excitation energies and at the neutron binding energy equally well. Voinov *et al.* [5] stated recently that for Ni and Co nuclei the CT formula works better up to 20 MeV.

For the newly extracted level-density parameters a, E_1 and T, E_0 we determined, as in Ref. [4], global formulas [Eqs. (19)–(22)] that describe them as functions of Z and A. These global formulas reproduce the empirical parameters reasonably well and use only quantities from mass tables. This fact indicates that the statistical properties of excited nuclei are determined by few parameters and that the ground-state masses of nuclei already contain the basic properties.

ACKNOWLEDGMENTS

This work was partially funded by the Romanian National Authority for Scientific Research under PNCDI2 programme, Contract No. ID-117/01.10.2007.

APPENDIX

TABLE I. Experimental data used for the determination of the spin-cutoff parameter σ (Secs. II and III) and of the level density parameters (Sec. IV). The third column concerns the spin window for the low-energy levels (within the energy range specified by the second column) and gives the range of the completeness. The values in columns 2 to 4 differ sometimes from those in the similar Table I of Ref. [4], because only levels with spins were accepted and new data was available. Also, the deuteron pairing given now is that defined by formula (12). The spin of the neutron resonances is restricted in a window, usually $J \pm 1/2$, where J is the spin of the neutron capturing nucleus (for an $\ell = 0$ captured neutron). Some of the light nuclei (with mass below 40) for which the neutron resonances either were not measured or cannot be measured (with blank columns 8 and 9) were nevertheless used in our fits because their level schemes are well known up to high excitation energies.

Nucleus	Energy range (MeV)	Spin window ($\hbar$)	Number of levels	Deuteron pairing Pa'[a] (MeV)	Shell correction S (MeV)	n binding energy (MeV)	Spin ($\hbar$)	Density (at n binding energy) (per MeV)
^{18}F	6.88	0–4	47	−6.763	1.586	9.149		
^{19}F	7.94	1/2–11/2	52	−1.781	1.792	10.432		
^{20}F	4.09	0–4	21	−4.384	4.131	6.601	0–1	6(2)
^{20}Ne	13.97	0–6	104	4.886	−3.358	16.865		
^{23}Na	6.95	1/2–9/2	30	0.068	0.174	12.419		
^{24}Na	4.57	0–4	32	−3.700	2.854	6.960	1–2	11(3)
^{24}Mg	11.19	0–4	44	5.237	−4.325	16.531		
^{25}Mg	7.51	1/2–9/2	51	−0.170	−0.339	7.331	1/2	2(1)
^{26}Mg	8.58	0–4	48	3.580	−1.503	11.093	2–3	23(9)
^{27}Mg	5.18	1/2–7/2	20	0.800	0.726	6.443	1/2	4(1)
^{26}Al	8.19	0–5	160	−5.501	0.305	11.366		
^{27}Al	7.59	1/2–11/2	54	−0.347	−1.256	13.058		
^{28}Al	5.01	1–4	37	−3.473	1.206	7.725	2–3	22(7)
^{28}Si	11.59	0–6	65	5.287	−6.129	17.180		
^{29}Si	8.00	1/2–9/2	41	1.076	−2.943	8.474	1/2	5(2)
^{30}Si	8.99	0–4	51	3.855	−3.133	10.609	0–1	3(1)
^{30}P	6.00	0–5	41	−3.552	−2.060	11.319		
^{31}P	7.15	1/2–9/2	44	0.200	−2.564	12.312		
^{32}P	4.21	0–4	25	−2.877	0.132	7.936	0–1	13(4)
^{32}S	8.35	0–4	36	3.694	−5.181	15.042		
^{33}S	4.95	1/2–11/2	22	−0.141	−1.877	8.642	1/2	7(2)
^{34}S	6.49	0–4	25	3.018	−2.470	11.417	1–2	37(14)
^{35}S	3.81	1/2–7/2	10	−0.203	0.332	6.986	1/2	5(2)
^{36}Cl	3.97	1–3	21	−2.801	0.848	8.580	1–2	44(11)
^{38}Cl	2.76	0–3	12	−3.052	3.523	6.108	1–2	67(18)
^{38}Ar	6.78	0–6	40	3.186	−1.557	11.838		
^{40}Ar	4.50	0–6	22	2.630	1.510	9.869		
^{41}Ar	1.88	1/2–5/2	6	−0.129	3.901	6.099	1/2	14(4)
^{40}K	3.49	1–4	32	−3.094	2.287	7.800	1–2	67(22)
^{41}K	3.59	1/2–9/2	34	−0.266	2.594	10.095	7/2–9/2	400(43)
^{42}K	1.38	1–6	16	−3.231	4.603	7.534	1–2	67(22)
^{40}Ca	8.12	0–6	48	4.385	−4.209	15.643		
^{41}Ca	4.10	1/2–11/2	26	0.140	−0.168	8.363	1/2	31(4)
^{43}Ca	2.62	1/2–7/2	14	0.095	2.459	7.933	1/2	50(13)
^{44}Ca	3.67	0–4	11	3.079	1.076	11.131	3–4	556(93)
^{45}Ca	2.53	1/2–7/2	11	0.349	2.628	7.415	1/2	41(6)
^{46}Sc	2.08	2–5	31	−3.219	3.554	8.761	3–4	769(59)
^{47}Ti	2.80	1/2–9/2	23	0.420	0.945	8.880	1/2	40(7)
^{48}Ti	4.11	0–4	21	2.998	−0.562	11.627	2–3	570(80)
^{49}Ti	2.67	1/2–7/2	12	0.292	0.680	8.142	1/2	55(9)
^{50}Ti	4.95	0–4	13	3.458	−1.570	10.939	3–4	250(50)
^{51}Ti	3.24	1/2–7/2	12	0.527	0.088	6.372	1/2	8(4)
^{51}V	3.39	1/2–9/2	16	0.280	−0.309	11.051	1/2	430(110)
^{52}V	2.40	1–4	20	−2.738	1.277	7.311	3–4	240(40)
^{51}Cr	3.02	1/2–9/2	21	0.126	−1.124	9.261	1/2	75(7)
^{53}Cr	3.00	1/2–7/2	14	0.327	−0.902	7.939	1/2	23(2)

TABLE I. (*Continued.*)

Nucleus	Energy range (MeV)	Spin window ($\hbar$)	Number of levels	Deuteron pairing Pa'[a] (MeV)	Shell correction S (MeV)	n binding energy (MeV)	Spin ($\hbar$)	Density (at n binding energy) (per MeV)
^{54}Cr	4.13	0–4	20	2.757	−1.527	9.719	1–2	130(13)
^{55}Cr	2.72	1/2–9/2	17	0.438	0.694	6.246	1/2	16(2)
^{56}Mn	1.39	1–3	16	−2.633	1.013	7.270	2–3	430(80)
^{55}Fe	2.61	1/2–9/2	15	0.463	−3.274	9.298	1/2	56(7)
^{57}Fe	2.70	1/2–9/2	28	0.209	−1.293	7.646	1/2	39(4)
^{58}Fe	3.91	0–4	21	2.874	−1.882	10.045	0–1	154(24)
^{59}Fe	2.17	1/2–7/2	15	0.470	0.395	6.581	1/2	39(8)
^{60}Co	2.23	2–5	35	−2.799	0.805	7.492	3–4	800(96)
^{59}Ni	2.54	1/2–9/2	16	0.490	−3.637	8.999	1/2	75(5)
^{60}Ni	3.89	0–4	21	3.150	−4.020	11.388	1–2	500(180)
^{61}Ni	2.60	1/2–9/2	23	0.315	−1.460	7.820	1/2	73(5)
^{62}Ni	3.53	0–4	18	3.209	−2.274	10.597	1–2	480(34)
^{63}Ni	1.46	1/2–9/2	9	0.430	0.098	6.838	1/2	63(12)
^{65}Ni	1.93	1/2–9/2	12	0.546	1.143	6.098	1/2	51(8)
^{64}Cu	1.61	0–3	26	−2.397	0.903	7.916	1–2	1050(100)
^{66}Cu	1.98	0–3	28	−2.293	2.138	7.066	1–2	770(70)
^{65}Zn	1.96	1/2–9/2	22	−0.318	0.103	7.979	1/2	280(13)
^{67}Zn	1.79	1/2–9/2	21	−0.415	1.601	7.052	1/2	216(26)
^{68}Zn	3.50	0–4	21	2.423	0.407	10.198	2–3	2500(380)
^{69}Zn	2.09	1/2–5/2	18	−0.312	2.425	6.482	1/2	180(14)
^{71}Zn	2.42	1/2–5/2	14	−0.391	2.936	5.834	1/2	140(15)
^{70}Ga	1.27	1–4	17	−2.386	3.349	7.654	0–1	2860(490)
^{72}Ga	0.86	0–4	15	−2.904	4.389	6.520	1–2	2630(420)
^{71}Ge	1.61	1/2–7/2	29	−0.234	2.778	7.416	1/2	1120(300)
^{73}Ge	1.16	1/2–9/2	27	−0.289	3.395	6.783	1/2	667(130)
^{74}Ge	3.06	0–4	36	2.983	1.562	10.196	4–5	16100(3900)
^{75}Ge	1.43	1/2–9/2	23	0.048	2.967	6.505	1/2	330(110)
^{77}Ge	1.39	1/2–9/2	15	0.163	1.999	6.072	1/2	220(70)
^{76}As	0.69	0–4	40	−2.933	4.518	7.328	1–2	13000(1350)
^{75}Se	1.21	1/2–9/2	29	0.073	3.070	8.028	1/2	2940(690)
^{77}Se	1.01	1/2–7/2	16	0.049	3.240	7.419	1/2	1540(240)
^{78}Se	2.96	0–6	30	2.935	1.425	10.498	0–1	9100(2500)
^{79}Se	1.39	1/2–9/2	30	−0.028	2.709	6.963	1/2	500(125)
^{81}Se	2.19	1/2–9/2	23	0.065	1.334	6.701	1/2	500(200)
^{83}Se	1.72	1/2–5/2	15	−0.231	−0.099	5.818	1/2	200(100)
^{80}Br	0.78	1–5	38	−2.918	4.029	7.892	1–2	21300(2300)
^{82}Br	0.98	1–5	20	−2.599	2.672	7.593	1–2	9500(1400)
^{79}Kr	1.18	1/2–11/2	33	0.096	2.712	8.334	1/2	4000(1300)
^{81}Kr	1.45	1/2–9/2	25	0.122	2.608	7.873	1/2	3570(770)
^{84}Kr	3.43	0–5	21	2.309	−0.659	10.521	4–5	5000(2500)
^{85}Kr	2.51	1/2–9/2	23	−0.323	−0.030	7.121	1/2	1000(100)
^{86}Rb	1.83	0–5	25	−2.429	0.445	8.651	2–3	5900(1000)
^{88}Rb	1.80	0–4	20	−1.993	−0.123	6.082	1–2	560(90)
^{85}Sr	1.99	1/2–9/2	29	0.054	0.996	8.530	1/2	3100(1200)
^{87}Sr	3.07	1/2–9/2	31	−0.054	−0.823	8.428	1/2	385(118)
^{88}Sr	4.31	0–5	18	3.303	−3.489	11.113	4–5	3400(1000)
^{89}Sr	3.14	1/2–9/2	18	0.738	−1.787	6.359	1/2	42(5)
^{90}Y	1.82	0–3	14	−1.700	−0.992	6.857	0–1	270(30)
^{91}Zr	2.94	1/2–9/2	25	0.435	−2.163	7.195	1/2	167(39)
^{92}Zr	3.30	0–4	23	2.026	−2.071	8.635	2–3	1820(330)
^{93}Zr	2.19	1/2–5/2	12	0.552	−0.454	6.734	1/2	286(65)
^{94}Zr	2.71	0–5	12	2.058	−0.689	8.221	2–3	6250(590)
^{95}Zr	2.38	1/2–5/2	11	0.743	0.482	6.462	1/2	310(80)
^{97}Zr	2.27	1/2–9/2	10	1.178	1.293	5.575	1/2	77(18)
^{94}Nb	0.93	2–5	17	−2.256	0.733	7.228	4–5	12500(1600)

TABLE I. (*Continued.*)

Nucleus	Energy range (MeV)	Spin window ($\hbar$)	Number of levels	Deuteron pairing Pa'[a] (MeV)	Shell correction S (MeV)	n binding energy (MeV)	Spin ($\hbar$)	Density (at n binding energy) (per MeV)
^{93}Mo	2.55	1/2–9/2	19	0.477	−3.057	8.070	1/2	370(70)
^{95}Mo	1.38	1/2–7/2	11	0.493	−0.984	7.369	1/2	758(103)
^{96}Mo	2.60	0–4	18	2.394	−1.149	9.154	2–3	9520(910)
^{97}Mo	1.57	1/2–11/2	30	0.486	0.653	6.821	1/2	950(180)
^{98}Mo	2.63	0–6	34	2.300	0.279	8.643	2–3	13300(3600)
^{99}Mo	1.27	1/2–9/2	26	−0.005	2.276	5.925	1/2	1000(200)
^{101}Mo	0.99	1/2–9/2	34	0.049	3.433	5.398	1/2	1250(230)
^{100}Tc	0.72	2–5	31	−2.587	3.014	6.764	4–5	83300(9000)
^{100}Ru	2.60	0–6	32	2.616	−0.994	9.673	2–3	40000(6400)
^{102}Ru	2.05	0–4	13	2.615	0.397	9.220	2–3	55600(9300)
^{103}Ru	0.78	1/2–11/2	29	0.168	2.360	6.232	1/2	1820(500)
^{105}Ru	0.85	1/2–7/2	26	0.197	2.962	5.910	1/2	3330(830)
^{104}Rh	0.61	1–3	33	−2.550	2.837	6.999	0–1	31300(3900)
^{105}Pd	0.95	1/2–9/2	20	0.199	0.785	7.094	1/2	4170(520)
^{106}Pd	2.48	0–4	23	2.625	0.006	9.561	2–3	97100(4700)
^{107}Pd	0.79	1/2–11/2	16	0.083	1.922	6.536	1/2	3700(1200)
^{108}Pd	2.43	0–6	22	2.613	0.826	9.228	2–3	90900(7400)
^{109}Pd	0.68	1/2–7/2	20	0.063	2.490	6.154	1/2	5490(1000)
^{111}Pd	0.59	1/2–9/2	13	−0.018	2.678	5.726	1/2	6700(2200)
^{108}Ag	0.69	0–4	29	−2.524	2.260	7.271	0–1	45500(8300)
^{110}Ag	0.39	1–3	15	−2.590	3.093	6.809	0–1	66200(6100)
^{107}Cd	1.29	1/2–7/2	19	0.206	−1.177	7.924	1/2	7410(1920)
^{109}Cd	1.18	1/2–7/2	15	0.108	0.193	7.327	1/2	8300(2100)
^{111}Cd	1.28	1/2–7/2	24	0.211	1.016	6.976	1/2	6450(830)
^{112}Cd	3.09	0–6	70	2.564	0.003	9.394	0–1	50000(10000)
^{113}Cd	1.29	1/2–7/2	29	0.169	1.538	6.540	1/2	5260(690)
^{114}Cd	2.82	0–4	36	2.582	0.271	9.043	0–1	40300(4200)
^{115}Cd	1.10	1/2–7/2	18	0.100	1.614	6.141	1/2	4260(630)
^{117}Cd	1.36	1/2–7/2	18	0.078	1.256	5.777	1/2	2560(590)
^{114}In	0.91	2–5	14	−2.482	1.870	7.274	4–5	76900(17700)
^{116}In	0.90	3–4	19	−2.588	2.150	6.785	4–5	105300(5500)
^{113}Sn	1.87	1/2–7/2	21	0.633	−0.775	7.743	1/2	6370(2110)
^{115}Sn	2.00	1/2–7/2	13	1.027	−0.453	7.546	1/2	3500(1300)
^{116}Sn	3.98	0–4	65	3.242	−1.397	9.563	0–1	21700(6600)
^{117}Sn	1.68	1/2–7/2	15	0.891	−0.022	6.943	1/2	2630(900)
^{118}Sn	2.75	0–4	14	3.317	−1.324	9.327	0–1	18200(1700)
^{119}Sn	1.36	1/2–7/2	11	0.798	−0.068	6.484	1/2	2080(390)
^{120}Sn	2.47	0–4	11	3.323	−1.717	9.108	0–1	11100(2500)
^{121}Sn	0.96	1/2–7/2	7	0.738	−0.702	6.170	1/2	610(74)
^{123}Sn	1.08	1/2–7/2	7	0.772	−1.885	5.946	1/2	600(180)
^{125}Sn	2.20	1/2–7/2	35	0.835	−3.551	5.733	1/2	200(48)
^{122}Sb	0.65	1–5	25	−2.483	1.065	6.806	2–3	76900(11800)
^{124}Sb	0.53	2–5	19	−2.383	−0.006	6.467	3–4	41700(5200)
^{123}Te	1.57	1/2–7/2	31	−0.044	0.416	6.929	1/2	7580(860)
^{124}Te	3.11	0–4	64	2.404	−1.301	9.424	0–1	58800(10400)
^{125}Te	2.19	1/2–7/2	71	−0.081	−0.432	6.569	1/2	5260(550)
^{126}Te	2.90	0–6	41	2.385	−2.370	9.114	0–1	26300(3500)
^{127}Te	2.20	1/2–7/2	71	−0.098	−1.739	6.288	1/2	1820(330)
^{129}Te	2.20	1/2–7/2	46	−0.069	−3.516	6.082	1/2	1350(270)
^{131}Te	2.59	1/2–7/2	40	−0.048	−5.739	5.929	1/2	670(220)
^{128}I	0.43	1–5	23	−2.235	−0.144	6.826	2–3	66700(13300)
^{130}I	0.39	2–5	22	−2.202	−1.641	6.500	3–4	33300(3300)
^{129}Xe	1.00	1/2–9/2	20	0.174	−0.733	6.909	1/2	4000(1600)
^{130}Xe	2.37	0–6	19	2.433	−2.568	9.256	0–1	26300(3500)
^{131}Xe	1.04	1/2–9/2	13	0.128	−2.005	6.605	1/2	4350(1130)

TABLE I. (*Continued.*)

Nucleus	Energy range (MeV)	Spin window ($\hbar$)	Number of levels	Deuteron pairing Pa'[a] (MeV)	Shell correction S (MeV)	n binding energy (MeV)	Spin ($\hbar$)	Density (at n binding energy) (per MeV)
^{132}Xe	3.09	2–6	34	2.367	−4.021	8.937	1–2	20400(6300)
^{133}Xe	1.36	1/2–7/2	13	0.130	−3.778	6.434	1/2	1330(420)
^{135}Xe	2.12	1/2–9/2	16	0.199	−6.046	6.364	1/2	625(230)
^{137}Xe	1.72	1/2–9/2	9	0.134	−6.414	4.026	1/2	77(36)
^{134}Cs	0.63	2–5	26	−2.193	−1.847	6.892	3–4	47600(4500)
^{135}Cs	0.62	5/2–7/2	4	−0.099	−3.807	8.762	7/2–9/2	62500(11700)
^{131}Ba	1.17	1/2–9/2	20	0.186	0.023	7.494	1/2	17240(3000)
^{133}Ba	1.36	1/2–7/2	20	0.198	−0.912	7.190	1/2	9090(2900)
^{135}Ba	0.99	1/2–7/2	9	0.263	−2.292	6.972	1/2	2700(260)
^{136}Ba	2.44	0–5	18	2.179	−4.237	9.108	1–2	25000(3800)
^{137}Ba	2.36	1/2–7/2	16	0.313	−4.220	6.906	1/2	826(81)
^{138}Ba	3.25	0–4	22	2.930	−6.142	8.612	1–2	3850(740)
^{139}Ba	2.23	1/2–7/2	24	0.170	−4.406	4.723	1/2	53(8)
^{139}La	1.79	1/2–9/2	16	0.651	−4.184	8.778	9/2–11/2	31250(5860)
^{140}La	0.80	0–5	23	−2.079	−2.536	5.161	3–4	4500(800)
^{137}Ce	1.19	1/2–5/2	10	0.140	−1.243	7.482	1/2	20000(8000)
^{141}Ce	2.21	1/2–9/2	23	0.286	−3.026	5.428	1/2	320(50)
^{142}Ce	2.40	0–5	20	2.000	−3.268	7.170	3–4	15400(4700)
^{143}Ce	1.23	1/2–9/2	14	0.325	−1.712	5.145	1/2	910(410)
^{142}Pr	0.75	1–4	12	−2.125	−1.389	5.843	2–3	9100(1600)
^{143}Nd	2.50	1/2–9/2	48	0.360	−2.243	6.124	1/2	1160(110)
^{144}Nd	2.70	0–5	33	2.125	−2.445	7.817	3–4	28600(4100)
^{145}Nd	1.60	1/2–9/2	27	0.376	−0.816	5.755	1/2	2220(250)
^{146}Nd	2.29	0–4	35	2.117	−1.225	7.565	3–4	58800(10400)
^{147}Nd	0.99	1/2–7/2	16	0.300	0.416	5.292	1/2	3450(590)
^{148}Nd	1.69	0–4	20	2.253	−0.203	7.333	2–3	286000(139000)
^{149}Nd	0.80	1/2–7/2	23	−0.044	1.257	5.039	1/2	6450(830)
^{151}Nd	0.69	1/2–7/2	18	0.082	0.912	5.335	1/2	6060(550)
^{148}Pm	0.22	1–2	4	−2.122	1.788	5.895	3–4	192000(44000)
^{145}Sm	2.20	1/2–11/2	27	0.398	−2.024	6.757	1/2	1490(130)
^{148}Sm	2.40	0–6	39	2.212	−0.734	8.141	3–4	196000(19000)
^{149}Sm	1.06	1/2–11/2	27	0.288	0.995	5.871	1/2	10000(2000)
^{150}Sm	2.11	0–6	42	2.174	0.384	7.987	3–4	476000(68000)
^{151}Sm	0.54	1/2–9/2	32	−0.140	1.943	5.596	1/2	21700(3800)
^{152}Sm	1.78	0–6	33	2.093	0.625	8.258	3–4	962000(139000)
^{153}Sm	0.49	1/2–9/2	23	−0.044	1.484	5.868	1/2	20800(2200)
^{155}Sm	0.99	1/2–5/2	19	0.121	0.543	5.807	1/2	8770(1150)
^{152}Eu	0.35	1–4	64	−2.489	3.157	6.307	2–3	1370000(131000)
^{153}Eu	0.74	1/2–9/2	22	0.044	1.870	8.550	5/2–7/2	1790000(320000)
^{154}Eu	0.49	1–5	74	−1.911	2.477	6.442	2–3	910000(165000)
^{155}Eu	1.11	1/2–9/2	29	0.126	1.164	8.151	5/2–7/2	1087000(142000)
^{156}Eu	0.39	0–5	27	−1.486	1.455	6.340	2–3	232600(81100)
^{153}Gd	0.69	1/2–9/2	41	−0.067	2.087	6.247	1/2	71400(15000)
^{155}Gd	1.09	1/2–5/2	32	0.005	1.713	6.435	1/2	69400(7200)
^{156}Gd	2.13	0–6	67	1.931	0.333	8.536	1–2	588000(69000)
^{157}Gd	0.80	1/2–9/2	25	0.147	0.920	6.360	1/2	33300(6700)
^{158}Gd	2.06	0–6	56	1.727	−0.276	7.937	1–2	204000(21000)
^{159}Gd	0.88	1/2–9/2	26	0.099	0.319	5.943	1/2	12200(900)
^{161}Gd	0.84	1/2–11/2	16	0.185	−0.282	5.635	1/2	5000(500)
^{160}Tb	0.39	0–5	27	−1.597	1.274	6.375	1–2	238000(17000)
^{157}Dy	0.57	1/2–7/2	18	0.131	1.725	6.969	1/2	208000(70000)
^{159}Dy	0.64	1/2–11/2	21	0.185	1.202	6.833	1/2	45500(23000)
^{161}Dy	0.87	1/2–5/2	20	0.098	0.695	6.454	1/2	37000(6900)
^{162}Dy	1.90	0–6	44	1.770	−0.547	8.197	2–3	417000(35000)
^{163}Dy	0.96	1/2–7/2	26	0.200	−0.062	6.271	1/2	16100(1300)

TABLE I. (*Continued.*)

Nucleus	Energy range (MeV)	Spin window ($\hbar$)	Number of levels	Deuteron pairing Pa'[a] (MeV)	Shell correction S (MeV)	n binding energy (MeV)	Spin ($\hbar$)	Density (at n binding energy) (per MeV)
^{164}Dy	2.01	0–5	36	1.594	−1.161	7.658	2–3	147000(13000)
^{165}Dy	0.81	1/2–9/2	24	0.172	−0.512	5.716	1/2	6700(500)
^{166}Ho	0.65	0–7	45	−1.408	0.297	6.244	3–4	238000(28000)
^{163}Er	0.71	1/2–9/2	25	0.103	1.121	6.903	1/2	125000(31000)
^{165}Er	1.01	1/2–9/2	38	0.062	0.553	6.650	1/2	47600(9100)
^{167}Er	0.90	1/2–11/2	30	0.204	−0.233	6.436	1/2	26300(2100)
^{168}Er	2.10	0–6	65	1.556	−1.234	7.771	3–4	238000(17000)
^{169}Er	0.86	1/2–11/2	23	0.176	−0.659	6.003	1/2	10000(1000)
^{171}Er	0.71	1/2–9/2	13	0.192	−1.001	5.682	1/2	6800(930)
^{170}Tm	0.47	0–6	23	−1.326	0.177	6.592	0–1	118000(10000)
^{171}Tm	1.04	1/2–9/2	19	−0.025	−0.626	7.486	1/2–3/2	256000(66000)
^{169}Yb	0.84	1/2–11/2	26	0.179	0.367	6.867	1/2	125000(47000)
^{170}Yb	2.05	0–6	41	1.739	−0.742	8.470	3–4	625000(16000)
^{171}Yb	1.09	1/2–13/2	35	0.229	−0.191	6.615	1/2	30300(5500)
^{172}Yb	1.76	0–6	33	1.572	−1.237	8.019	0–1	173000(14000)
^{173}Yb	1.13	1/2–9/2	15	0.363	−0.820	6.367	1/2	14200(530)
^{174}Yb	1.64	0–4	11	1.564	−1.686	7.465	2–3	128000(15000)
^{175}Yb	1.13	1/2–9/2	21	0.375	−1.092	5.822	1/2	6200(700)
^{177}Yb	1.00	1/2–9/2	16	0.299	−1.229	5.566	1/2	5400(560)
^{176}Lu	0.86	0–7	58	−1.308	−0.046	6.288	3–4	333000(45000)
^{177}Lu	1.11	1/2–9/2	24	−0.197	−0.601	7.073	13/2–15/2	364000(112000)
^{175}Hf	1.00	1/2–13/2	27	0.179	0.025	6.708	1/2	55600(15400)
^{177}Hf	0.93	1/2–13/2	27	0.121	−0.370	6.383	1/2	33300(7800)
^{178}Hf	1.95	0–6	53	1.282	−1.196	7.626	3–4	417000(52000)
^{179}Hf	1.29	1/2–9/2	36	0.055	−0.676	6.099	1/2	17500(1800)
^{180}Hf	1.44	0–4	18	1.400	−1.623	7.388	4–5	217000(14000)
^{181}Hf	1.41	1/2–9/2	33	0.230	−1.053	5.695	1/2	10600(1700)
^{181}Ta	0.63	1/2–11/2	9	0.022	−0.809	7.577	1/2–3/2	833000(139000)
^{182}Ta	0.79	2–5	35	−1.313	−0.332	6.063	3–4	238000(17000)
^{183}Ta	0.58	5/2–9/2	7	−0.103	−0.900	6.934	9/2–11/2	286000(57000)
^{181}W	1.00	1/2–9/2	21	0.165	−0.621	6.681	1/2	50000(17500)
^{183}W	1.06	1/2–11/2	25	0.235	−1.067	6.191	1/2	16700(1700)
^{184}W	1.54	0–6	25	1.524	−1.840	7.412	0–1	83300(6900)
^{185}W	1.40	1/2–9/2	51	0.132	−1.129	5.754	1/2	14300(1400)
^{187}W	1.10	1/2–7/2	37	0.216	−1.368	5.467	1/2	11800(1100)
^{186}Re	0.70	1–5	35	−1.490	−0.466	6.179	2–3	323000(31000)
^{188}Re	0.53	1–5	26	−1.590	−0.740	5.872	2–3	244000(18000)
^{187}Os	0.69	1/2–11/2	23	0.079	−1.085	6.290	1/2	34500(3600)
^{188}Os	1.97	0–4	25	1.794	−2.244	7.990	0–1	250000(38000)
^{189}Os	0.61	1/2–7/2	18	0.024	−1.506	5.920	1/2	21300(2700)
^{190}Os	1.49	0–6	17	1.780	−2.809	7.792	1–2	294000(35000)
^{191}Os	0.64	1/2–9/2	22	0.136	−2.245	5.759	1/2	14300(2000)
^{193}Os	0.55	1/2–7/2	12	0.373	−3.234	5.583	1/2	8700(800)
^{192}Ir	0.30	0–3	21	−1.900	−1.483	6.198	1–2	400000(80000)
^{193}Ir	1.09	1/2–7/2	28	−0.061	−2.837	7.772	1/2	1429000(408000)
^{194}Ir	0.68	0–4	57	−1.733	−2.649	6.067	1–2	142900(40800)
^{193}Pt	0.61	1/2–7/2	17	−0.161	−2.449	6.255	1/2	45500(17000)
^{195}Pt	0.70	1/2–7/2	20	−0.041	−3.719	6.105	1/2	5000(2000)
^{196}Pt	2.10	0–6	50	1.590	−5.292	7.922	0–1	55600(9300)
^{197}Pt	0.60	1/2–7/2	14	0.030	−4.949	5.846	1/2	2860(820)
^{199}Pt	0.65	1/2–7/2	12	0.056	−6.157	5.556	1/2	2940(780)
^{198}Au	0.68	0–3	27	−1.492	−4.920	6.512	1–2	60600(3300)
^{199}Hg	0.76	1/2–7/2	12	0.385	−6.211	6.664	1/2	9500(3200)
^{200}Hg	2.20	0–3	28	1.721	−7.703	8.028	0–1	12500(4700)

TABLE I. (*Continued.*)

Nucleus	Energy range (MeV)	Spin window ($\hbar$)	Number of levels	Deuteron pairing Pa'[a] (MeV)	Shell correction S (MeV)	n binding energy (MeV)	Spin ($\hbar$)	Density (at n binding energy) (per MeV)
^{201}Hg	0.65	1/2–7/2	11	0.235	−7.556	6.230	1/2	1540(360)
^{202}Hg	1.91	0–4	25	1.538	−9.090	7.754	1–2	11100(3700)
^{204}Tl	0.69	0–4	15	−1.218	−8.932	6.656	0–1	3600(640)
^{206}Tl	2.00	0–6	24	−0.966	−10.818	6.504	0–1	182(50)
^{205}Pb	2.26	1/2–9/2	29	0.862	−9.699	6.732	1/2	500(125)
^{207}Pb	3.52	1/2–11/2	15	1.412	−11.869	6.738	1/2	31(6)
^{208}Pb	5.30	0–10	71	3.226	−13.137	7.368	0–1	26(6)
^{209}Pb	3.69	1/2–15/2	34	1.168	−11.126	3.937	1/2	3(1)
^{210}Bi	1.48	2–7	19	−1.267	−9.173	4.605	4–5	250(44)
^{227}Ra	0.53	1/2–5/2	16	0.103	1.271	4.561	1/2	32300(6300)
^{229}Th	0.49	1/2–7/2	20	0.050	1.147	5.257	1/2	200000(120000)
^{230}Th	1.20	0–6	27	1.556	0.306	6.794	2–3	1613000(312000)
^{231}Th	1.09	1/2–7/2	48	0.303	1.006	5.118	1/2	104000(16000)
^{233}Th	0.79	1/2–7/2	38	0.389	1.019	4.786	1/2	60200(2200)
^{233}Pa	0.50	1/2–11/2	28	−0.121	0.979	6.529	3/2–5/2	1330000(270000)
^{234}Pa	0.20	0–4	8	−1.392	1.530	5.220	1–2	1670000(280000)
^{233}U	0.60	1/2–9/2	19	0.315	0.575	5.762	1/2	217000(33000)
^{234}U	1.50	0–6	37	1.515	−0.147	6.845	2–3	1818000(165000)
^{235}U	0.96	1/2–13/2	61	0.261	0.545	5.297	1/2	83300(5600)
^{236}U	1.17	0–6	27	1.452	−0.144	6.545	3–4	2326000(108000)
^{237}U	0.68	1/2–13/2	25	0.428	0.456	5.126	1/2	66700(4500)
^{238}U	1.16	0–6	22	1.520	−0.100	6.154	0–1	286000(65000)
^{239}U	0.90	1/2–7/2	25	0.376	0.562	4.806	1/2	48100(700)
^{237}Np	0.76	1/2–11/2	29	−0.118	0.470	6.580	1/2–3/2	1670000(170000)
^{238}Np	0.40	1–5	36	−1.168	0.923	5.488	2–3	1754000(92000)
^{239}Np	0.37	1/2–11/2	16	−0.138	0.519	6.215	3/2–5/2	2440000(600000)
^{239}Pu	0.83	1/2–9/2	21	0.313	−0.001	5.646	1/2	111000(12000)
^{240}Pu	1.32	0–6	29	1.334	−0.512	6.534	0–1	455000(10000)
^{241}Pu	0.79	1/2–9/2	23	0.287	0.141	5.242	1/2	80600(4600)
^{242}Pu	1.19	0–6	18	1.379	−0.402	6.310	0–1	1370000(150000)
^{243}Pu	0.93	1/2–11/2	29	0.325	0.202	5.034	1/2	74000(8200)
^{245}Pu	0.58	1/2–9/2	8	0.409	0.314	4.771	1/2	52600(8300)
^{242}Am	0.51	0–6	39	−1.179	0.565	5.538	2–3	1724000(119000)
^{243}Am	0.35	3/2–13/2	13	−0.195	0.176	6.365	1/2–3/2	2500000(500000)
^{244}Am	0.59	0–4	42	−1.211	0.659	5.366	2–3	1370000(113000)
^{243}Cm	0.14	1/2–9/2	6	0.192	−0.265	5.693	1/2	71400(15300)
^{244}Cm	1.19	0–3	9	1.265	−0.878	6.801	2–3	1333000(267000)
^{245}Cm	0.80	1/2–11/2	25	0.327	−0.340	5.520	1/2	84700(8600)
^{246}Cm	1.72	0–3	32	1.362	−0.867	6.458	0–1	769000(118000)
^{247}Cm	0.59	1/2–9/2	14	0.339	−0.217	5.156	1/2	33300(5600)
^{248}Cm	1.31	0–4	12	1.579	−0.750	6.213	4–5	714000(150000)
^{249}Cm	0.59	1/2–9/2	18	0.441	0.094	4.713	1/2	35700(6400)
^{250}Bk	0.24	1–6	20	−1.238	0.549	4.970	3–4	909000(83000)
^{250}Cf	1.40	0–6	28	1.515	−1.321	6.625	4–5	1429000(204000)
^{251}Cf	0.73	1/2–11/2	26	0.297	−0.462	5.108	1/2	83300(14000)

[a]Quantity Pa', as defined by Eq. (12).

TABLE II. Experimental level density parameters for the BSFG and CT models [Eqs. (1)–(5)], determined from fits to the data sets specified in Table I (Appendix), by using the energy-dependent spin-cutoff parameter defined with the empirical formula (16).

Nucleus	BSFG		CT	
	a (δa) (MeV^{-1})	E_1 (δE_1) (MeV)	T (δT) (MeV)	E_0 (δE_0) (MeV)
^{18}F	2.63(44)	−2.25(154)	2.29(42)	−2.23(180)
^{19}F	2.21(37)	−2.98(182)	2.88(56)	−3.70(246)
^{20}F	3.01(42)	−2.41(118)	2.16(41)	−3.03(180)
^{20}Ne	2.29(24)	1.69(126)	2.85(31)	0.87(146)
^{23}Na	3.13(76)	0.10(188)	2.06(54)	−0.38(231)
^{24}Na	3.03(36)	−2.70(105)	2.04(51)	−2.75(224)
^{24}Mg	2.86(41)	2.94(124)	2.25(28)	2.53(120)
^{25}Mg	2.68(37)	−1.83(131)	2.48(44)	−2.68(196)
^{26}Mg	3.25(40)	1.19(89)	2.01(29)	0.69(122)
^{27}Mg	4.93(58)	1.25(64)	1.37(19)	0.68(81)
^{26}Al	2.86(28)	−3.20(106)	2.39(22)	−4.18(128)
^{27}Al	2.95(39)	−0.89(114)	2.16(32)	−1.19(145)
^{28}Al	3.50(22)	−1.91(66)	1.97(19)	−2.74(107)
^{28}Si	3.07(46)	3.21(115)	2.07(24)	3.05(104)
^{29}Si	3.27(53)	0.62(111)	2.20(40)	−0.58(168)
^{30}Si	2.75(33)	0.22(117)	2.34(34)	−0.12(153)
^{30}P	3.05(32)	−1.79(101)	2.14(26)	−2.14(126)
^{31}P	3.45(63)	0.10(127)	1.82(33)	0.03(135)
^{32}P	3.62(33)	−1.69(072)	1.89(31)	−2.30(143)
^{32}S	3.19(59)	1.39(135)	1.93(34)	1.48(134)
^{33}S	3.99(32)	0.09(61)	1.69(22)	−0.33(103)
^{34}S	3.91(35)	1.32(62)	1.72(21)	0.99(93)
^{35}S	4.56(70)	0.33(83)	1.38(23)	0.38(96)
^{36}Cl	3.96(31)	−1.63(66)	1.78(26)	−2.39(136)
^{38}Cl	6.33(55)	−0.13(45)	1.07(14)	−0.31(73)
^{38}Ar	4.36(57)	1.61(80)	1.45(18)	1.61(80)
^{40}Ar	4.80(78)	0.69(84)	1.30(20)	0.72(83)
^{41}Ar	5.57(53)	−0.64(63)	1.23(17)	−0.96(97)
^{40}K	4.61(23)	−1.61(46)	1.56(21)	−2.33(120)
^{41}K	5.37(11)	−0.64(27)	1.44(08)	−1.70(62)
^{42}K	3.99(40)	−3.73(88)	1.89(28)	−5.14(157)
^{40}Ca	4.40(65)	2.58(84)	1.39(19)	2.80(79)
^{41}Ca	5.62(23)	0.39(33)	1.26(10)	−0.02(58)
^{43}Ca	5.78(37)	−0.48(40)	1.26(11)	−1.08(65)
^{44}Ca	5.97(26)	1.24(41)	1.26(7)	0.72(56)
^{45}Ca	6.31(34)	0.04(42)	1.15(9)	−0.50(61)
^{46}Sc	5.69(15)	−2.29(31)	1.43(9)	−3.72(71)
^{47}Ti	4.89(24)	−1.29(43)	1.55(13)	−2.37(83)
^{48}Ti	5.56(19)	0.76(33)	1.39(7)	−0.12(54)
^{49}Ti	6.09(30)	−0.14(39)	1.20(9)	−0.60(66)
^{50}Ti	5.95(31)	2.14(40)	1.23(9)	1.74(63)
^{51}Ti	5.47(81)	0.02(64)	1.21(21)	−0.08(84)
^{51}V	6.84(31)	0.78(32)	1.17(6)	0.01(46)
^{52}V	6.00(28)	−1.27(34)	1.24(9)	−1.91(59)
^{51}Cr	5.57(19)	−0.57(34)	1.36(7)	−1.36(55)
^{53}Cr	5.30(25)	−0.49(44)	1.36(10)	−1.01(69)
^{54}Cr	5.46(22)	0.70(38)	1.36(8)	0.05(56)
^{55}Cr	5.93(29)	−0.53(35)	1.21(12)	−1.01(69)
^{56}Mn	5.96(31)	−2.37(44)	1.33(10)	−3.49(77)
^{55}Fe	5.27(20)	−0.80(40)	1.43(11)	−1.56(76)
^{57}Fe	5.50(21)	−1.31(33)	1.38(8)	−2.26(57)
^{58}Fe	5.90(23)	0.62(32)	1.29(7)	−0.09(49)
^{59}Fe	6.41(37)	−0.80(35)	1.15(9)	−1.40(58)
^{60}Co	6.89(20)	−1.55(24)	1.17(8)	−2.60(54)
^{59}Ni	5.69(18)	−0.76(34)	1.34(8)	−1.53(69)
^{60}Ni	5.80(35)	0.54(36)	1.34(9)	−0.24(55)
^{61}Ni	6.30(17)	−0.76(27)	1.22(8)	−1.54(53)
^{62}Ni	6.12(18)	0.60(32)	1.27(6)	−0.13(51)
^{63}Ni	6.84(36)	−0.73(37)	1.10(9)	−1.29(62)
^{65}Ni	7.77(39)	−0.17(31)	0.96(7)	−0.67(47)
^{64}Cu	6.84(20)	−2.00(28)	1.21(6)	−3.22(56)
^{66}Cu	7.55(22)	−1.37(24)	1.07(5)	−2.28(41)
^{65}Zn	7.44(24)	−0.87(32)	1.08(6)	−1.69(57)
^{67}Zn	7.94(23)	−0.83(22)	1.00(6)	−1.54(45)
^{68}Zn	7.95(24)	0.99(22)	1.01(4)	0.35(35)
^{69}Zn	8.56(27)	−0.54(24)	0.91(5)	−1.16(40)
^{71}Zn	10.21(40)	0.36(23)	0.76(4)	−0.15(35)
^{70}Ga	9.49(38)	−0.94(23)	0.89(5)	−1.72(41)
^{72}Ga	9.36(32)	−1.40(23)	0.88(6)	−2.16(50)
^{71}Ge	9.40(40)	−0.88(19)	0.90(5)	−1.82(33)
^{73}Ge	9.00(33)	−1.32(20)	0.94(5)	−2.34(38)
^{74}Ge	9.70(31)	0.71(15)	0.90(3)	−0.21(25)
^{75}Ge	8.73(55)	−1.00(24)	0.92(7)	−1.79(40)
^{77}Ge	9.05(58)	−0.68(24)	0.86(7)	−1.22(40)
^{76}As	9.60(20)	−2.23(17)	0.95(3)	−3.71(31)
^{75}Se	9.74(30)	−1.07(16)	0.91(5)	−2.19(38)
^{77}Se	9.69(26)	−1.00(20)	0.88(5)	−1.93(44)
^{78}Se	9.74(35)	0.79(16)	0.89(3)	−0.04(26)
^{79}Se	8.70(39)	−1.24(21)	0.97(5)	−2.26(37)
^{81}Se	10.42(36)	0.10(16)	0.77(4)	−0.46(29)
^{83}Se	9.44(39)	−0.66(24)	0.84(5)	−1.24(40)
^{80}Br	9.96(20)	−1.92(16)	0.93(3)	−3.29(32)
^{82}Br	10.05(27)	−1.23(19)	0.86(3)	−2.11(33)
^{79}Kr	9.72(42)	−1.18(17)	0.92(5)	−2.39(32)
^{81}Kr	10.66(33)	−0.58(15)	0.82(3)	−1.43(27)
^{84}Kr	8.57(30)	1.05(20)	0.97(4)	0.44(32)
^{85}Kr	11.49(38)	0.53(15)	0.71(3)	0.09(27)
^{86}Rb	8.83(26)	−0.77(19)	0.96(4)	−1.56(33)
^{88}Rb	8.85(34)	−0.78(22)	0.88(5)	−1.25(36)
^{85}Sr	10.16(54)	−0.30(17)	0.85(5)	−1.08(29)
^{87}Sr	8.60(40)	0.24(20)	0.94(7)	−0.39(38)
^{88}Sr	8.48(39)	1.95(23)	0.96(5)	1.48(34)
^{89}Sr	8.63(38)	0.70(25)	0.84(5)	0.50(35)
^{90}Y	7.91(30)	−0.92(30)	0.99(6)	−1.48(49)
^{91}Zr	9.12(44)	0.41(23)	0.85(5)	0.03(33)
^{92}Zr	9.09(31)	0.89(20)	0.88(4)	0.37(30)
^{93}Zr	9.91(47)	0.12(24)	0.80(5)	−0.36(38)
^{94}Zr	11.70(32)	1.35(20)	0.71(3)	0.92(27)
^{95}Zr	10.97(58)	0.50(24)	0.71(5)	0.21(35)
^{97}Zr	10.67(64)	0.68(25)	0.68(5)	0.61(33)
^{94}Nb	10.52(27)	−1.24(19)	0.83(3)	−2.10(35)
^{93}Mo	8.92(33)	0.19(22)	0.90(5)	−0.29(41)
^{95}Mo	9.78(27)	−0.42(22)	0.84(6)	−0.98(47)
^{96}Mo	10.27(19)	0.71(16)	0.82(3)	0.13(30)
^{97}Mo	10.55(34)	−0.55(15)	0.80(4)	−1.32(29)

TABLE II. (*Continued.*)

Nucleus	BSFG		CT	
	a (δa) (MeV^{-1})	E_1 (δE_1) (MeV)	T (δT) (MeV)	E_0 (δE_0) (MeV)
^{98}Mo	11.28(40)	0.66(14)	0.77(3)	−0.07(23)
^{99}Mo	11.65(40)	−0.66(15)	0.72(3)	−1.33(26)
^{101}Mo	12.24(40)	−0.97(13)	0.71(3)	−1.80(25)
^{100}Tc	13.29(31)	−1.37(13)	0.71(2)	−2.49(24)
^{100}Ru	11.38(25)	0.68(12)	0.79(2)	−0.11(21)
^{102}Ru	12.41(26)	0.77(15)	0.72(3)	0.19(28)
^{103}Ru	11.28(47)	−1.22(16)	0.79(4)	−2.27(30)
^{105}Ru	12.96(48)	−0.93(13)	0.69(3)	−1.80(25)
^{104}Rh	12.39(23)	−1.79(14)	0.78(4)	−3.10(37)
^{105}Pd	11.83(26)	−0.79(15)	0.75(3)	−1.63(29)
^{106}Pd	12.83(14)	0.85(11)	0.71(2)	0.17(22)
^{107}Pd	12.52(56)	−0.73(16)	0.70(4)	−1.45(29)
^{108}Pd	13.43(20)	1.01(12)	0.68(2)	0.33(19)
^{109}Pd	13.36(34)	−0.93(14)	0.68(4)	−1.81(32)
^{111}Pd	15.04(66)	−0.62(14)	0.59(3)	−1.22(27)
^{108}Ag	13.23(29)	−1.29(13)	0.72(3)	−2.32(30)
^{110}Ag	14.18(26)	−1.43(16)	0.68(4)	−2.48(42)
^{107}Cd	11.88(40)	−0.52(15)	0.76(3)	−1.31(28)
^{109}Cd	13.01(44)	−0.38(14)	0.68(3)	−1.01(27)
^{111}Cd	13.07(27)	−0.48(12)	0.69(2)	−1.23(22)
^{112}Cd	13.61(28)	1.02(07)	0.69(2)	0.17(16)
^{113}Cd	13.43(29)	−0.52(11)	0.67(2)	−1.29(21)
^{114}Cd	13.90(18)	1.05(9)	0.67(2)	0.30(17)
^{115}Cd	13.98(35)	−0.43(13)	0.63(2)	−1.02(23)
^{117}Cd	14.16(52)	−0.22(12)	0.60(3)	−0.67(23)
^{114}In	13.52(38)	−0.72(16)	0.68(4)	−1.43(34)
^{116}In	14.13(22)	−1.09(15)	0.67(3)	−2.09(35)
^{113}Sn	12.85(55)	0.12(15)	0.69(3)	−0.54(24)
^{115}Sn	13.00(65)	0.53(18)	0.66(4)	0.04(27)
^{116}Sn	13.03(40)	1.66(9)	0.69(2)	0.89(15)
^{117}Sn	13.00(60)	0.15(16)	0.66(4)	−0.36(27)
^{118}Sn	12.88(24)	1.32(14)	0.68(2)	0.87(25)
^{119}Sn	13.26(43)	0.06(17)	0.64(3)	−0.40(29)
^{120}Sn	12.40(39)	1.19(17)	0.70(3)	0.78(29)
^{121}Sn	11.43(41)	−0.29(24)	0.71(5)	−0.71(52)
^{123}Sn	12.26(65)	−0.03(25)	0.67(7)	−0.45(54)
^{125}Sn	10.62(49)	−0.29(18)	0.76(4)	−0.87(29)
^{122}Sb	13.68(27)	−1.19(12)	0.69(3)	−2.08(30)
^{124}Sb	12.89(27)	−1.42(16)	0.72(4)	−2.36(36)
^{123}Te	13.73(25)	−0.34(10)	0.66(2)	−1.06(19)
^{124}Te	13.87(29)	0.98(8)	0.68(2)	0.09(14)
^{125}Te	14.22(24)	−0.10(8)	0.64(2)	−0.90(14)
^{126}Te	13.36(24)	1.04(9)	0.68(2)	0.35(16)
^{127}Te	12.64(38)	−0.38(11)	0.69(3)	−1.16(18)
^{129}Te	12.97(46)	−0.10(12)	0.65(3)	−0.69(19)
^{131}Te	12.89(43)	0.27(12)	0.64(3)	−0.20(18)
^{128}I	12.97(33)	−1.57(15)	0.73(4)	−2.64(37)
^{130}I	11.88(24)	−1.95(18)	0.79(6)	−3.18(55)
^{129}Xe	12.34(66)	−0.72(16)	0.72(4)	−1.47(29)
^{130}Xe	13.00(25)	0.89(13)	0.69(2)	0.34(22)
^{131}Xe	13.51(49)	−0.36(15)	0.64(4)	−0.85(31)
^{132}Xe	12.18(57)	0.98(13)	0.72(3)	0.32(21)
^{133}Xe	12.19(59)	−0.32(18)	0.69(4)	−0.77(31)
^{135}Xe	12.55(74)	0.44(18)	0.65(4)	0.12(26)

TABLE II. (*Continued.*)

Nucleus	BSFG		CT	
	a (δa) (MeV^{-1})	E_1 (δE_1) (MeV)	T (δT) (MeV)	E_0 (δE_0) (MeV)
^{137}Xe	14.76(50)	0.56(21)	0.49(5)	0.51(27)
^{134}Cs	12.38(21)	−1.55(14)	0.75(4)	−2.62(35)
^{135}Cs	11.40(41)	−0.79(33)	0.80(5)	−1.52(64)
^{131}Ba	13.99(32)	−0.38(11)	0.66(2)	−1.04(22)
^{133}Ba	13.61(56)	−0.33(13)	0.66(3)	−0.97(24)
^{135}Ba	12.26(31)	−0.42(19)	0.70(3)	−0.93(35)
^{136}Ba	12.34(28)	0.83(14)	0.72(2)	0.31(25)
^{137}Ba	12.20(32)	0.49(17)	0.68(3)	0.09(26)
^{138}Ba	11.02(35)	1.17(16)	0.76(3)	0.71(25)
^{139}Ba	10.84(52)	−0.07(21)	0.70(5)	−0.35(32)
^{139}La	11.60(31)	0.05(17)	0.77(4)	−0.58(41)
^{140}La	12.32(38)	−1.17(16)	0.69(5)	−1.79(37)
^{137}Ce	14.48(69)	−0.23(16)	0.63(3)	−0.78(30)
^{141}Ce	13.50(47)	0.47(14)	0.59(3)	0.18(21)
^{142}Ce	14.40(53)	0.94(12)	0.59(3)	0.57(21)
^{143}Ce	14.87(95)	−0.01(16)	0.57(7)	−0.44(40)
^{142}Pr	12.73(66)	−0.98(32)	0.68(9)	−1.53(72)
^{143}Nd	14.17(29)	0.47(10)	0.60(2)	−0.04(16)
^{144}Nd	14.17(27)	0.96(10)	0.62(3)	0.43(22)
^{145}Nd	15.03(33)	0.03(11)	0.58(2)	−0.49(22)
^{146}Nd	15.11(35)	0.64(09)	0.60(2)	0.02(16)
^{147}Nd	15.93(44)	−0.35(11)	0.55(2)	−0.81(21)
^{148}Nd	18.27(90)	0.62(10)	0.51(3)	0.11(17)
^{149}Nd	17.06(37)	−0.60(10)	0.53(2)	−1.19(18)
^{151}Nd	16.07(31)	−0.67(11)	0.56(2)	−1.31(21)
^{148}Pm	16.95(70)	−1.05(27)	0.56(4)	−1.75(50)
^{145}Sm	13.18(27)	0.38(12)	0.64(2)	−0.04(22)
^{148}Sm	16.30(22)	0.88(07)	0.58(1)	0.27(13)
^{149}Sm	16.47(44)	−0.33(09)	0.55(2)	−0.90(17)
^{150}Sm	17.69(29)	0.72(07)	0.55(1)	0.06(12)
^{151}Sm	17.02(35)	−0.93(09)	0.56(3)	−1.79(22)
^{152}Sm	17.84(24)	0.53(07)	0.55(1)	−0.16(14)
^{153}Sm	16.43(26)	−0.91(10)	0.58(2)	−1.75(24)
^{155}Sm	16.03(32)	−0.53(12)	0.57(3)	−1.19(31)
^{152}Eu	18.39(20)	−1.54(7)	0.58(3)	−2.80(27)
^{153}Eu	16.24(26)	−0.63(9)	0.63(3)	−1.53(29)
^{154}Eu	17.85(31)	−1.36(7)	0.58(3)	−2.54(23)
^{155}Eu	16.68(24)	−0.35(8)	0.60(2)	−1.14(21)
^{156}Eu	16.23(65)	−1.23(12)	0.61(3)	−2.19(23)
^{153}Gd	17.89(38)	−0.78(7)	0.55(2)	−1.66(19)
^{155}Gd	18.08(32)	−0.50(10)	0.54(2)	−1.31(21)
^{156}Gd	17.19(19)	0.50(5)	0.58(1)	−0.34(13)
^{157}Gd	16.99(41)	−0.55(9)	0.56(2)	−1.26(20)
^{158}Gd	16.62(11)	0.44(6)	0.58(1)	−0.32(13)
^{159}Gd	16.21(24)	−0.57(9)	0.57(2)	−1.24(22)
^{161}Gd	15.80(31)	−0.41(11)	0.56(2)	−0.89(21)
^{160}Tb	16.74(23)	−1.20(10)	0.59(1)	−2.14(19)
^{157}Dy	18.54(62)	−0.59(10)	0.54(2)	−1.38(20)
^{159}Dy	16.29(88)	−0.66(12)	0.59(3)	−1.43(23)
^{161}Dy	16.89(35)	−0.60(10)	0.57(3)	−1.36(24)
^{162}Dy	16.75(19)	0.41(7)	0.58(1)	−0.33(13)
^{163}Dy	16.01(24)	−0.57(10)	0.59(2)	−1.31(18)
^{164}Dy	16.35(27)	0.48(8)	0.58(1)	−0.16(14)
^{165}Dy	15.58(25)	−0.66(10)	0.59(2)	−1.34(21)

TABLE II. (*Continued.*)

Nucleus	BSFG		CT	
	a (δa) (MeV^{-1})	E_1 (δE_1) (MeV)	T (δT) (MeV)	E_0 (δE_0) (MeV)
^{166}Ho	16.85(27)	−0.97(8)	0.58(1)	−1.83(15)
^{163}Er	17.90(47)	−0.58(9)	0.55(2)	−1.36(17)
^{165}Er	16.92(39)	−0.56(8)	0.57(2)	−1.33(15)
^{167}Er	16.61(22)	−0.52(8)	0.57(1)	−1.23(16)
^{168}Er	16.51(18)	0.39(6)	0.58(1)	−0.38(12)
^{169}Er	15.93(24)	−0.54(9)	0.58(2)	−1.16(21)
^{171}Er	16.14(37)	−0.48(12)	0.55(2)	−0.98(23)
^{170}Tm	16.77(24)	−0.96(10)	0.58(2)	−1.76(19)
^{171}Tm	16.89(47)	−0.28(10)	0.57(2)	−0.89(19)
^{169}Yb	18.28(66)	−0.41(8)	0.53(3)	−1.09(20)
^{170}Yb	16.96(22)	0.55(11)	0.58(1)	−0.16(17)
^{171}Yb	16.71(37)	−0.39(8)	0.57(2)	−1.05(17)
^{172}Yb	17.26(15)	0.42(7)	0.56(1)	−0.24(16)
^{173}Yb	16.72(33)	−0.11(14)	0.54(2)	−0.55(26)
^{174}Yb	16.91(31)	0.62(14)	0.54(3)	0.23(34)
^{175}Yb	16.24(32)	−0.25(10)	0.55(2)	−0.75(18)
^{177}Yb	16.64(33)	−0.25(11)	0.53(2)	−0.67(20)
^{176}Lu	17.88(29)	−0.74(7)	0.55(1)	−1.55(13)
^{177}Lu	18.78(60)	−0.18(8)	0.52(2)	−0.77(16)
^{175}Hf	17.41(60)	−0.34(8)	0.54(2)	−0.92(16)
^{177}Hf	17.52(47)	−0.38(9)	0.54(2)	−0.99(16)
^{178}Hf	17.86(16)	0.43(6)	0.55(2)	−0.27(18)
^{179}Hf	17.40(24)	−0.25(7)	0.54(2)	−0.86(16)
^{180}Hf	16.94(25)	0.27(11)	0.56(3)	−0.29(34)
^{181}Hf	18.04(40)	−0.04(8)	0.51(1)	−0.57(14)
^{181}Ta	18.72(45)	−0.26(11)	0.52(2)	−0.73(24)
^{182}Ta	17.68(22)	−0.81(8)	0.55(1)	−1.60(15)
^{183}Ta	16.71(45)	−0.52(16)	0.57(3)	−1.09(32)
^{181}W	17.68(69)	−0.28(10)	0.54(3)	−0.86(22)
^{183}W	16.98(26)	−0.31(8)	0.54(1)	−0.86(16)
^{184}W	17.24(23)	0.31(8)	0.55(1)	−0.25(15)
^{185}W	17.91(26)	−0.25(6)	0.52(1)	−0.87(12)
^{187}W	17.83(28)	−0.45(8)	0.52(1)	−1.12(15)
^{186}Re	18.19(25)	−0.82(8)	0.54(1)	−1.59(15)
^{188}Re	18.26(25)	−0.90(9)	0.53(1)	−1.64(17)
^{187}Os	17.34(27)	−0.60(9)	0.55(1)	−1.29(18)
^{188}Os	18.72(33)	0.73(8)	0.52(1)	0.12(14)
^{189}Os	17.10(34)	−0.73(11)	0.56(2)	−1.44(21)
^{190}Os	17.83(25)	0.47(9)	0.54(2)	−0.05(18)
^{191}Os	16.87(35)	−0.70(10)	0.56(2)	−1.41(20)
^{193}Os	16.63(34)	−0.62(13)	0.55(2)	−1.23(25)
^{192}Ir	17.61(45)	−1.47(13)	0.59(2)	−2.61(25)
^{193}Ir	20.84(71)	−0.21(7)	0.50(2)	−0.92(14)
^{194}Ir	16.60(58)	−1.29(10)	0.60(2)	−2.31(19)
^{193}Pt	17.68(74)	−0.70(12)	0.55(3)	−1.40(22)
^{195}Pt	14.01(73)	−1.01(16)	0.66(4)	−1.85(29)
^{196}Pt	15.91(27)	0.40(7)	0.60(2)	−0.29(15)
^{197}Pt	13.64(58)	−1.00(17)	0.66(4)	−1.75(34)
^{199}Pt	14.61(58)	−0.77(15)	0.61(3)	−1.36(29)

TABLE II. (*Continued.*)

Nucleus	BSFG		CT	
	a (δa) (MeV^{-1})	E_1 (δE_1) (MeV)	T (δT) (MeV)	E_0 (δE_0) (MeV)
^{198}Au	14.49(20)	−1.37(12)	0.67(3)	−2.39(30)
^{199}Hg	14.79(61)	−0.58(15)	0.62(3)	−1.22(29)
^{200}Hg	13.24(22)	0.16(12)	0.70(3)	−0.57(25)
^{201}Hg	12.21(47)	−0.99(20)	0.73(4)	−1.72(39)
^{202}Hg	12.52(51)	0.01(14)	0.72(3)	−0.63(25)
^{204}Tl	11.38(37)	−1.43(21)	0.79(4)	−2.27(37)
^{206}Tl	8.58(49)	−0.90(25)	0.93(6)	−1.30(39)
^{205}Pb	11.12(50)	−0.13(16)	0.75(4)	−0.66(25)
^{207}Pb	9.65(46)	1.29(25)	0.79(7)	1.08(44)
^{208}Pb	8.47(52)	1.77(26)	0.86(6)	1.70(31)
^{209}Pb	8.03(36)	0.42(55)	0.84(1)	0.56(59)
^{210}Bi	9.79(46)	−0.96(24)	0.80(1)	−1.28(63)
^{227}Ra	22.66(59)	−0.55(09)	0.42(2)	−1.10(17)
^{229}Th	23.40(87)	−0.54(10)	0.42(3)	−1.12(18)
^{230}Th	22.45(43)	0.24(6)	0.45(1)	−0.30(12)
^{231}Th	24.44(39)	−0.18(4)	0.40(1)	−0.76(11)
^{233}Th	23.91(50)	−0.38(11)	0.41(2)	−0.97(31)
^{233}Pa	20.46(43)	−0.71(7)	0.50(1)	−1.50(15)
^{234}Pa	25.66(57)	−0.64(11)	0.40(2)	−1.17(22)
^{233}U	23.23(40)	−0.33(7)	0.43(1)	−0.87(15)
^{234}U	23.17(21)	0.43(5)	0.44(1)	−0.12(12)
^{235}U	22.96(19)	−0.31(4)	0.43(1)	−0.93(10)
^{236}U	23.84(19)	0.28(6)	0.42(1)	−0.25(13)
^{237}U	23.22(24)	−0.29(6)	0.41(1)	−0.78(13)
^{238}U	23.31(32)	0.31(7)	0.42(1)	−0.16(13)
^{239}U	24.31(22)	−0.16(6)	0.39(2)	−0.62(18)
^{237}Np	22.56(26)	−0.35(6)	0.46(1)	−0.97(12)
^{238}Np	23.51(20)	−0.82(6)	0.44(1)	−1.58(15)
^{239}Np	22.91(55)	−0.56(8)	0.45(1)	−1.20(17)
^{239}Pu	22.77(45)	−0.20(9)	0.43(1)	−0.67(17)
^{240}Pu	23.08(16)	0.33(6)	0.43(1)	−0.18(12)
^{241}Pu	23.44(26)	−0.24(6)	0.41(1)	−0.70(12)
^{242}Pu	26.70(36)	0.47(7)	0.38(1)	0.07(11)
^{243}Pu	24.72(35)	−0.08(5)	0.39(1)	−0.50(10)
^{245}Pu	25.14(56)	−0.07(9)	0.37(1)	−0.32(18)
^{242}Am	23.92(21)	−0.65(5)	0.43(1)	−1.32(13)
^{243}Am	23.52(47)	−0.51(8)	0.44(1)	−1.11(17)
^{244}Am	23.86(27)	−0.71(6)	0.44(1)	−1.46(11)
^{243}Cm	20.02(52)	−0.78(16)	0.50(2)	−1.49(32)
^{244}Cm	22.56(52)	0.34(11)	0.43(2)	−0.01(30)
^{245}Cm	22.57(31)	−0.24(6)	0.43(1)	−0.73(12)
^{246}Cm	25.22(41)	0.55(5)	0.40(1)	0.00(10)
^{247}Cm	21.62(48)	−0.33(9)	0.44(2)	−0.78(17)
^{248}Cm	23.32(57)	0.49(0)	0.41(2)	0.16(25)
^{249}Cm	23.28(52)	−0.34(7)	0.41(1)	−0.79(15)
^{250}Bk	23.64(35)	−0.84(8)	0.43(1)	−1.50(15)
^{250}Cf	23.07(31)	0.42(6)	0.43(1)	−0.08(14)
^{251}Cf	23.86(46)	−0.27(6)	0.41(1)	−0.74(12)

[1] A. Gilbert and A. G. W. Cameron, Can. J. Phys. **43**, 1446 (1965); P. J. Brancazio and A. G. W. Cameron, *ibid.* **47**, 1029 (1969).
[2] T. von Egidy, A. N. Behkami, and H. H. Schmidt, Nucl. Phys. **A454**, 109 (1986).
[3] T. von Egidy, H. H. Schmidt, and A. N. Behkami, Nucl. Phys. **A481**, 189 (1988).
[4] T. von Egidy and D. Bucurescu, Phys. Rev. C **72**, 044311 (2005); **73**, 049901(E) (2006).
[5] A. V. Voinov, B. M. Oginni, S. M. Grimes, C. R. Brune, M. Guttormsen, A. V. Larsen, T. N. Massey, A. Schiller, and S. Siem, Phys. Rev. C **79**, 031301(R) (2009).
[6] A. V. Ignatyuk, G. N. Smirenkin, and A. S. Tishin, Yad. Fiz. **21**, 485 (1975) [Sov. J. Nucl. Phys. **21**, 255 (1975)].
[7] T. Ericson, Adv. Phys. **9**, 425 (1960).
[8] W. Dilg, W. Schantl, H. Vonach, and M. Uhl, Nucl. Phys. **A217**, 269 (1973).
[9] S. M. Grimes, J. D. Anderson, J. W. McClure, B. A. Pohl, and C. Wong, Phys. Rev. C **10**, 2373 (1974).
[10] A. S. Iljinov, M. V. Mebel, N. Bianchi, E. De Sanctis, C. Guaraldo, V. Lucherini, V. Muccifora, E. Polli, A. R. Reolon, and P. Rossi, Nucl. Phys. **A543**, 517 (1992).
[11] H. Zhongfu, H. Ping, S. Zongdi, and Z. Chunmei, Chin. J. Nucl. Phys. **13**, 147 (1991).
[12] T. Rauscher, F.-K. Thielemann, and K.-L. Kratz, Phys. Rev. C **56**, 1613 (1997).
[13] B. K. Agrawal, S. K. Samaddar, A. Ansari, and J. N. De, Phys. Rev. C **59**, 3109 (1999).
[14] P. L. Huang, S. M. Grimes, and T. N. Massey, Phys. Rev. C **62**, 024002 (2000).
[15] S. I. Al Quraishi, S. M. Grimes, T. N. Massey, and D. A. Ressler, Phys. Rev. C **67**, 015803 (2003).
[16] Y. Alhassid, S. Liu, and H. Nakada, Phys. Rev. Lett. **99**, 162504 (2007); Y. Alhassid (private communication).
[17] K. Kaneko and A. Schiller, Phys. Rev. C **75**, 044304 (2007).
[18] T. von Egidy and D. Bucurescu, Phys. Rev. C **78**, 051301(R) (2008).
[19] P. Hille, P. Sperr, M. Hille, K. Rudolph, W. Assmann, and D. Evers, Nucl. Phys. **A232**, 157 (1974).
[20] R. Fischer, G. Traxler, M. Uhl, and H. Vonach, Phys. Rev. C **30**, 72 (1984).
[21] S. M. Grimes, S. D. Bloom, H. K. Vonach, and R. F. Hausman Jr., Phys. Rev. C **27**, 2893 (1983).
[22] H. Vonach and J. R. Huizenga, Phys. Rev. **149**, 844 (1966).
[23] C. C. Lu, L. C. Vaz, and J. R. Huizenga, Nucl. Phys. **A190**, 229 (1972).
[24] A. V. Ignatyuk, J. L. Weil, S. Raman, and S. Kahane, Phys. Rev. C **47**, 1504 (1993).
[25] P. E. Garrett, H. Lehmann, J. Jolie, C. A. McGrath, Mingfang Yeh, W. Younes, and S. W. Yates, Phys. Rev. C **64**, 024316 (2001).
[26] P. E. Koehler, J. L. Ullmann, T. A. Bredeweg, J. M. O'Donnell, R. Reifert, R. S. Rundberg, D. J. Vieira, and J. M. Wouters, Phys. Rev. C **76**, 025804 (2007).
[27] J. Blachot, Nucl. Data Sheets, **92**, 455 (2001).
[28] J. M. Pearson, Hyperfine Interact. **132**, 59 (2001).
[29] G. Audi, http://amdc.in2p3.fr/masstables/Ame2003/rct7.mass03.
[30] G. Audi, A. H. Wapstra, and C. Thibault, Nucl. Phys. **A729**, 337 (2003).
[31] Evaluated Nuclear Structure Data File (ENSDF), maintained by the National Nuclear Data Center, Brookhaven National Laboratory (http://www.nndc.bnl.gov/ensdf).
[32] M. Gholami, M. Kildir, and A. N. Behkami, Phys. Rev. C **75**, 044308 (2007).
[33] U. Facchini and E. Saetta-Menichella, Energ. Nucl. (Milan) **15**, 54 (1967).
[34] B. Strohmaier, S. M. Grimes, and H. Satyanarayana, Phys. Rev. C **36**, 1604 (1987).
[35] M. Horoi, J. Kaiser, and V. Zelevinsky, Phys. Rev. C **67**, 054309 (2003).
[36] M. Horoi, M. Ghita, and V. A. Zelevinsky, Nucl. Phys. **A758**, 142c (2005).
[37] D. Bucurescu and T. von Egidy, Phys. Rev. C **72**, 067304 (2005).